ISSN 0801–9940
ISBN 82–553–1182–3

No. 99 - 1

Buckling of Stiffened Plates using a Shanley Model Approach

by

Eivind Steen

RESEARCH REPORT IN MECHANICS

UNIVERSITY OF OSLO
DEPARTMENT OF MATHEMATICS
MECHANICS DIVISION

1999

UNIVERSITETET I OSLO
MATEMATISK INSTITUTT
AVDELING FOR MEKANIKK

Buckling of Stiffened Plates using a Shanley Model Approach

EIVIND STEEN

Mechanics Division, Department of Mathematics, University of Oslo

Abstract - The Shanley model concept is used for simulating the elastic non-linear interaction between local buckling and overall buckling of thin-walled columns subjected to axial compression. The spring foundation is given a general macro material form for representing the local buckling response typical for thin walled cross-sections. For geometrically perfect columns, analytical post-buckling solutions are derived valid for and any cross-sectional shape. For geometrical imperfect columns a numerical procedure is proposed. The numerical method is based on a perturbation scheme with arc length control applied in an incremental procedure. It is demonstrated that the numerical method is able to trace unstable equilibrium paths with sharp peaks in the load-deflection space.

A simplified two-degree of freedom macro material model is developed, applicable for panels with open thin-walled stiffener profiles. Included in the cross-sectional macro model is plate buckling interacting with sideways/torsional buckling of the free stiffener outstand and buckling of the stiffener web plate.

The present analytical and numerical study verifies that the recognised reduced modulus is an important parameter in the non-linear elastic interaction between local and overall buckling of stiffened panels.

TABLE OF CONTENTS

1. INTRODUCTION

Buckling of thin-walled stiffened plates is a subject of continuous interest due to its relevance in the design process of technologically important structures such as ship, bridges and aerospace constructions. However, despite the huge amount of research results available on the subject, there are still many complicated items, which are not satisfactory treated in available design codes. The main items to be included in a physically consistent design model are the problems of mode interactions and unstable postbuckling behaviour, combined load effects, residual stress and heat affect zone effects and geometrical imperfection effects.

After the first warning made by Koiter and Skaloud (1963) against the optimum design philosophy of simultaneous local and overall buckling in stiffened panels, the topic of mode interactions has been on the agenda among engineers and scientist working in the field of structural stability. Van der Neut (1969) demonstrated that the procedure of designing panels having close or identical local and overall critical buckling loads lead to unstable postbuckling behaviour and increased imperfection sensitivity. Some time before, Graves-Smith (1967,1968) analysed the interaction between local and overall buckling in more general terms. Subsequently, a series of publications emerged focusing on the complex non-linear mode interaction effects and imperfection sensitivity, e.g. Koiter and Kuiken (1971), Thompsen and Lewis (1972), Tvergaard (1973).

Thompsen, Tulk and Walker (1974) studied the elastic mode interaction problem from a simplified and conceptual point of view using the Shanley model for a panel with stocky stiffeners and slender plating. Walker (1975) and Tulk and Walker (1976) showed theoretically, as well as by carefully performed laboratory experiments of small scale stiffened plates made of araldite, that the reduced modulus factor is an important parameter for the stability of the postbuckling response and consequently of the imperfection sensitivity. Ellinas and Croll (1977, 1979, 1981) adopted also the reduced modulus concept and calculated factors for the case of slender stiffener outstands (flat bar and bulb profiles in ship terminology).

The concept of reduced modulus factor in the elastic buckling theory, as developed by Thompsen, Walker, Croll and their co-workers, is in principle similar to the reduced modulus approach in the inelastic column buckling theory, originally developed by Considere (1891). Von Karman (1910) developed the inelastic buckling theory further, with subsequent important contributions by Shanley (1947) and Hutchinson (1973). The present work deals exclusively with the elastic buckling theory.

The objective of the present work is to develop a simplified numerical buckling model for tracing the complete non-linear elastic load-displacement curve of axially compressed stiffened plates. This includes the non-linear interaction effects between local and overall buckling modes together with geometrical imperfection effects. Such curves provide both strength and stiffness properties of compressed panels, which are vital parameters for overall strength assessment of larger structures. Geometrical imperfections both in local and overall modes are studied, but residual stresses and spread of material plasticity are left out. However, by controlling the magnitude of the stresses in critical locations in the panel, the present model can be used to assess the ultimate load bearing capacity using a first yield criterion.

First yield criteria used in combination with a non-linear elastic analysis are recognised and frequently used in simplified buckling models

Moreover, the objective was also to test out the feasibility of the perturbation method as a numerical tool for tracing continuous equilibrium curves. Details of the perturbation method used in an incremental scheme with arc length control are given in Steen (1998).

The present simplified buckling model is based on a generalised Shanley column formulation in which the local cross-sectional behaviour follows a two-dimensional spring law. The two-dimensional spring law is referred to as a local macro material model or just a macro model. It includes the local cross-sectional buckling behaviour in an integrated form coping exclusively with local non-linear geometrical effects. For coupling of the local and overall buckling effects, the Shanley model ensures a simple treatment of both the continuously changing cross-sectional bending and extensional stiffness properties and shift in neutral axis position with changing displacements. By using a two-dimensional macro model, the basic formulation developed can be used for any type of thin-walled cross-sectional shape, e.g. for open profiles, closed profiles, corrugated panels etc. The two-dimensional spring model can be extended to a six-dimensional model for use in the strength assessment of stiffened panels subjected to combined bi-axial and shear loads. However, the issue of combined loads is not addressed in detail in the present report.

In a non-linear analysis the overall cross-sectional bending and extensional stiffness properties are state dependent (load-dependent). This means that they will continuously change as the external applied load is increased. This effect is treated herein through an incremental updated numerical procedure. However, from a design code point of view, an even more simplified approach is to be preferred using a fixed set of reduced stiffness factors. Such a code model is currently under development, but is not described here.

This report develops specifically a macro material model for stiffened panels with open profiles, typically used in steel ships and offshore constructions. For these types of profiles it is of particular interest to study mode interactions between overall panel (column) buckling and local plate buckling and/or torsional sideways buckling of the stiffener.

A brief summary of the content is as follows. Chapter 2 describes a general formulation of the interactive buckling problem of columns using the Shanley model. The general section cross-sectional response is formulated as a non-linear macro material law without focussing on whether the cause of this non-linearity is due to cross-sectional buckling or pure material effects. Chapter 3 then describes a macro material law in which the local geometrical buckling parameters (q_i) of a general thin-walled cross-section become visible. For solving the non-linear geometrical problem, a perturbation procedure is formulated using an incremental approach with arc length control. Chapter 4 is more specific and develops the macro model for stiffened panels with open stiffener profiles of type T, L or flat bar, typically used in ship and offshore structures. The present report deals exclusively with stiffened panels subjected to pure axial loading for which a two-dimensional macro model is sufficient. Only some very general comments are given in Section 3.1, adapted to six-dimensional macro models to be used for combined in-plane load situations in stiffened panels.

Using the macro material law developed in Chapter 4 some numerical examples, using the incremental perturbation method, are presented in Chapter 5. Comparisons with some analytical and numerical solutions published in the literature are also given.

2. THE GENERAL SECTION SHANLEY COLUMN

2.1 General

After several decades of almost no interest in the problem of inelastic buckling of columns, Shanley(1947) presented a new approach to the topic and eliminated much of previous disagreements on whether to use the tangent or reduced modulus approach. Up to that time the reduced modulus load was accepted as the lowest buckling load of geometrically perfect straight columns made of inelastic material (von Karman (1910)). Shanley showed, using the simple two-spring model illustrated in Fig.1a, that the tangent modulus load was the minimum load at which the inelastic column starts to buckle. His findings were well documented, both by experiments and by incorporating the mentioned simple spring model with bi-linear inelastic material characteristics. In a discussion of Shanley's paper, von Karman agreed with the author's conclusions.

Chilver and Britvec (1964) studied in more depth the stability of columns in the inelastic region and developed a closed form solution for the postbuckling response. They confirmed that the tangent modulus load was the smallest possible buckling load and showed that the postbuckling equilibrium path approached asymptotically the reduced modulus load for increasing deflections (within the limit of moderate rotation theory and inelastic bi-linear material response). Hutchinson (1973) generalised the Shanley model by using a continuous spring model in order to simulate the uni-axially inelastic response of a real compact cross-section, Fig.1b. Using this model he studied the initial postbuckling behaviour in the inelastic region using asymptotic theories. Tvergaard and Needleman (1975) studied both with numerical and asymptotically methods the postbuckling behaviour of inelastic columns with and without geometrical imperfections.

Within inelastic column theory it can be stated that the reduced modulus load and tangent modulus load has a clear physical interpretation and it is recognised that the tangent modulus load represents the mathematically correct initial buckling load for perfect straight columns. However, for real columns with geometrical imperfections and residual stresses these theories have not been used to any large extent for design purposes. Numerical methods or semi-analytical methods like the Perry type of approach reviewed below have been preferred.

The publication by Ayrton and Perry (1886) is credited with being the first that focussed on the effect of geometrical imperfections and load eccentricities in the study on load bearing capability of columns (struts). The load causing the first yield at the extreme fibre in the critical section was called an elastic limit load. They showed that this load was a close approximation to the ultimate loads for a set of experiments carried out on different types of struts. Robertson(1925) developed this method further and showed good correlation with test results of initially crooked columns. The simplicity of the approach attracted the engineering

community dealing with design, and the Perry-Robertson approach is used in many international design codes dealing with buckling of columns as well as stiffened plates and cylindrical panels.

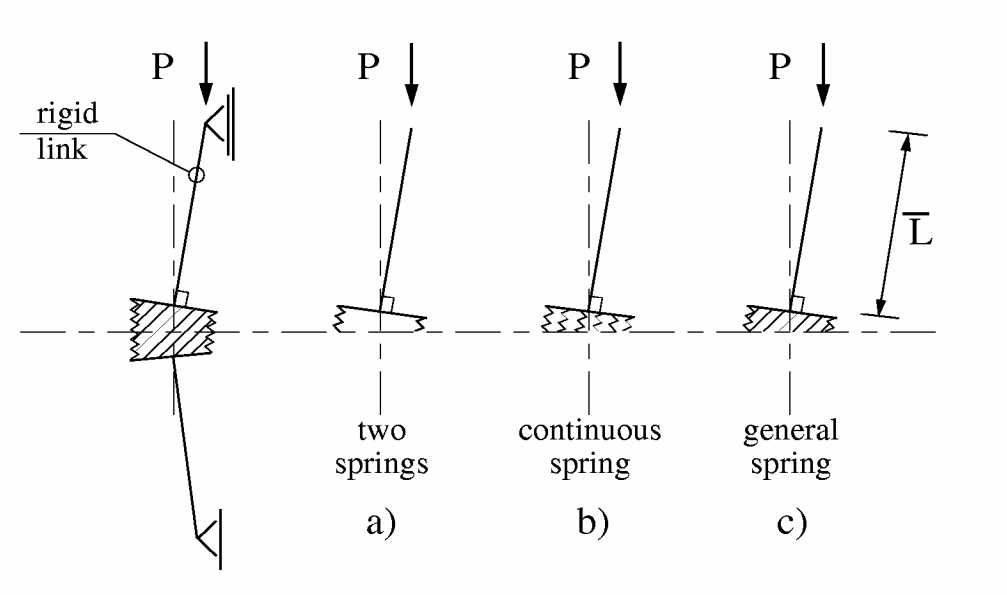

Fig.1 Shanley model, schematically

The Perry-Robertson model was developed for the buckling strength assessment of columns with compact cross-sections. In order to cope with the structural interaction between local cross-sectional buckling and overall column buckling, Thompsen, Tulk and Walker (1974) proposed to include the reduced modulus concept. They used the feature of reduced modulus in a general context, i.e. they realised that it could be used independently of whether it was the material or the local buckling of the cross-section that caused the local stiffness change. They made use of the accepted fact that the in-plane stiffness of a compressed geometrically perfect plate has an almost constant value beyond initial elastic buckling. To demonstrate the importance of this near constant postbuckling stiffness of plates they modelled a stocky stiffener with a flexible plate flange, whose effective stiffness was taken to be a fixed value (typically 50% of the unbuckled stiffness). For the case of the column buckling in the direction giving compression in the plate flange, they showed both theoretically and experimentally that the classical Euler column formula with the reduced bending stiffness $(EI)_R$ of the plate flange included, predicted a safe lower bound buckling strength value. In other words their approach predicted a lower bound estimate of the column buckling strength with a full elimination of the non-linear mode interaction effect. Ellinas et. al. (1977), Ellinas and Croll (1979) and Ellinas and Croll (1981) used the same approach for cases with slender stiffeners buckling in a sideways (torsional) mode.

The present work presents an extension of the reduced modulus approach to interactive elastic buckling of stiffened panels. A major assumption in the approach, as proposed by Thompsen, Walker, Croll and their co-workers, is that the reduced modulus factor is a fixed value. They assumed this fixed value to be independent of the plate dimensions, geometrical imperfections, and the level of the acting load. This approach can be classified as a lower

bound approach, which may be unduly conservative if the elastic local buckling load of the cross-section is well above the material yield stress. This is normally the case for ship and offshore constructions made of steel. However, the reduced modulus concept is a very intuitive and physically appealing approach and it can be extended for a more realistic strength assessment. By using a method for continuously updating the current macro stiffness properties, instead of using a fixed conservative value, significant improvements may be achieved. This is the main topic in the present report and the general section Shanley model illustrated in Fig.1c, provides for a simplified treatment.

The stiffened panel layout considered in this report is typical for ship structures. The panel rests on transverse girders providing rigid lateral supports as illustrated in Fig.2. The panel is wide compared to its length. This means that we can study the panel strength by considering an isolated unit. The *unit* consists of a single stiffener with an associated plate width equal to the full stiffener spacing s. This column model approach will give reasonable results for most geometries found in steel ships and offshore structures. It is commonly used in rules and guidelines issued by ship classification societies.

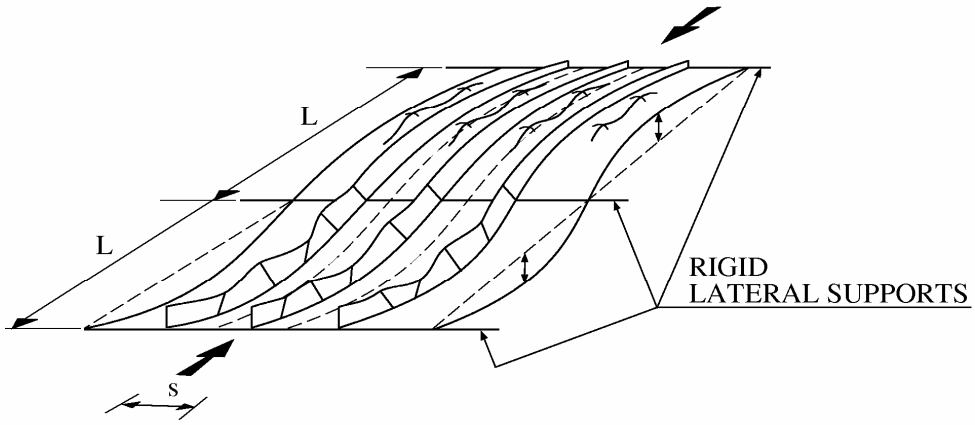

Fig.2 Stiffened panel with open profiles of flat bar (T or angle) type.
Overall Euler mode interacting with sideways(torsional) buckling of stiffeners and local buckling of plating

In the general Shanley model illustrated in Fig.1c, the spring represents the non-linear buckling response of the cross-section. Since the spring characteristics represent an integrated effect of local buckling and imperfection effects of the whole cross-section, the notion of *a macro material* has been introduced. In the limit of compact cross-sections, the spring characteristic represent the uni-axial linear elastic material stress-strain law. In the other limit, with very slender cross-sections prone to different types of local buckling, the macro model converge towards the lower bound method as proposed by Thompsen, Walker and their co-workers.

Material yielding is simply checked by evaluating the maximum membrane stress in critical locations (*hard corners)* at the column mid-span length. The problem of inelastic behaviour is not treated in depth in this report since this requires a more comprehensive approach. For

columns with compact sections such a comprehensive numerical model is documented in Steen and Andreassen (1995-I) and Steen and Andreassen (1995-II). This model handles the combination of axial load and lateral pressure for a multi-span beam-column and the spread of plasticity both in the cross-sections and along the length is included.

2.2 General formulation

The Shanley model in Fig.1c is reproduced with more definitions of parameters in Fig.3. The cross-sectional parameters N and M are the resultant axial force and moment, respectively, acting at the mid-span of the column. P is the external load always acting in the centroid of the column cross-section. The moment M is calculated about the cross-section centroid (X, Y, Z co-ordinate system placed as illustrated in Fig.3; centroid Y = 0, Z = 0). Note that a lowe case co-ordinate x, y, z system is used later in Chapter 4, with the y-axis laying in the plate middle-plane, Fig.8 ($Z = z\text{-}z_G$). The rotation θ of the rigid arm is due to the applied load P, while θ_0 is the initial (stress free imperfection) rotation for zero load.

The two global equilibrium equations of the Shanley model (Fig.3) are according to the theory of moderate rotations ($\sin\theta \approx \theta$) equal to

$$\begin{aligned} P - N &= 0 \\ P\bar{L}(\theta + \theta_0) - M &= 0 \end{aligned} \qquad (1)$$

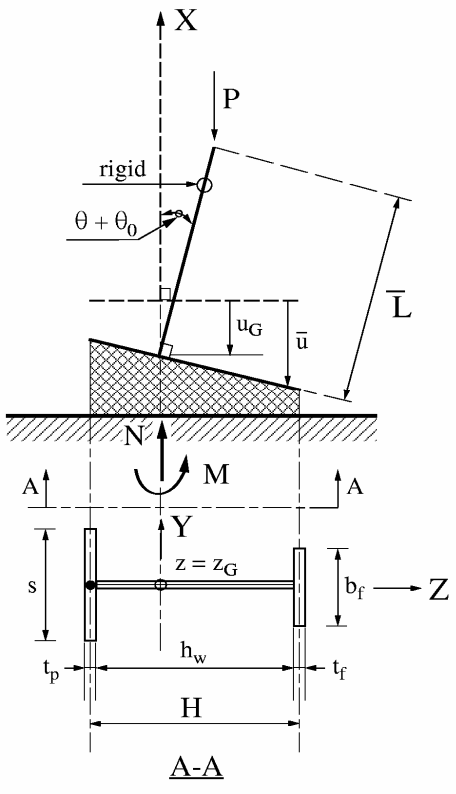

Fig.3 General section Shanley model
Example illustration: plate with attached T profile

A set of scaled displacement parameters are defined as

$$\begin{aligned} \varepsilon &= u_G / L \\ \kappa &= \theta / L \\ \kappa_0 &= \theta_0 / L \end{aligned} \qquad (2)$$

Here u_G is the axial displacement of the centroid. For convenience u_G is scaled with the full stiffener span L giving an axial average strain parameter ε (non-dimensional end-shortening). The rotation parameters θ and θ_0 are scaled similarly giving a measure κ (and κ_0) of the curvature of the column at mid-span. A positive ε is defined as a shortening of the column and a positive curvature κ gives compressive strains for material points located at $Z > 0$. Moreover, $\overline{L}$ is the symbol for the length of the rigid link of the Shanley model. The magnitude of $\overline{L}$ compared to the full continuous column length L is derived in Section 2.3.

The total cross-sectional forces N and M are defined as

$$\begin{aligned} N &= \iint_A \overline{\sigma}_x \, dX dZ \\ M &= \iint_A \overline{\sigma}_x \, Z \, dX dZ \end{aligned} \qquad (3)$$

The term total used here refers to total forces as opposed incremental forces, and the reference is always to the undeformed panel described in the rectangular co-ordinate system. The $\overline{\sigma}_x$ in Eq.(3) symbolises the axial stress in an arbitrary material point in the cross-section and it is defined as positive in compression (in buckling theory positive values are mostly used for critical loads etc.). When applied to thin-walled sections, the integrations in Eq.(3) will lead to sufficiently accurate estimates of the force and moment by letting $\overline{\sigma}_x$ be the membrane stress in each component plate (i.e. neglecting stress variations across a plate thickness in each component plate is a reasonable approximation).

By enforcing the Bernoulli-Euler hypothesis, the strain $\overline{\varepsilon}$ in an arbitrary point in the cross-section is related to the axial strain ε and curvature κ of the centroidal reference plane as

$$\overline{\varepsilon} = \varepsilon + Z \, \kappa \qquad (4)$$

Using Eq.(4) together with non-linear solutions for the membrane stress field in a thin-walled built up section (see Section 4.3.3), it can be shown that the membrane stress $\overline{\sigma}_x$ in a component plate are general functions of the strain ε and curvature κ of the centroid, i.e. expressed mathematically as

$$\overline{\sigma}_x = \overline{\sigma}_x(\varepsilon, \kappa) \qquad (5)$$

Eq.(5) can be interpreted as a general non-linear material law, which substituted into Eq.(3) gives the two-dimensional *macro material* functions on total form as

$$\begin{aligned} N &= N(\varepsilon, \kappa) \\ M &= M(\varepsilon, \kappa) \end{aligned} \qquad (6)$$

Note that in Eqs.(5)(6) $\overline{\sigma}_x$, N and M are used as symbols for the respective function as well as for the value of the function (stress, force and moment) even though this is not a rigorous mathematical notation.

Functions of this type can be derived for any column cross-sectional shape and both the material law and the cross-sectional buckling behaviour can be included into these functions. Details on how this can be done for a thin-walled cross-section with open profiles are given in Chapter 4. At this stage it is sufficient to accept that equations in form of Eq.(6) can be derived. These functions describe *a non-linear macro material model* for the cross-sectional behaviour, and it is immaterial at this stage whether the non-linearity is due to local cross-sectional buckling or due to non-linear elastic material behaviour.

By substituting Eq.(6) into Eq.(1), the cross-sectional forces N and M are eliminated in the equilibrium equations at the expense of the average strain ε and curvature κ. For completeness of notation the final form of the equilibrium equations are written as

$$\begin{aligned} P - N(\varepsilon, \kappa) &= 0 \\ P\, L\bar{L}(\kappa + \kappa_0) - M(\varepsilon, \kappa) &= 0 \end{aligned} \qquad (7)$$

Eq.(7) is the two overall equilibrium equations in the three unknowns P, ε and κ describing the non-linear geometrical response of an initially tilted Shanley column.

Since the two-dimensional *non-linear macro material law* described by Eq.(6) is central in the buckling model developed in this report, it is useful to discuss some of its main properties. By expanding Eq.(6) in a Taylor serie around any known equilibrium state I_s, the macro material law takes the form

$$\begin{aligned} \Delta N &= K_{11}\Delta\varepsilon + K_{12}\Delta\kappa + (1/2!)(K_{111}\Delta\varepsilon^2 + 2K_{112}\Delta\varepsilon\Delta\kappa + K_{122}\Delta\kappa^2) + \cdots \\ \Delta M &= K_{21}\Delta\varepsilon + K_{22}\Delta\kappa + (1/2!)(K_{211}\Delta\varepsilon^2 + 2K_{212}\Delta\varepsilon\Delta\kappa + K_{222}\Delta\kappa^2) + \cdots \end{aligned} \qquad (8)$$

Here the instantaneous spring stiffness coefficients K_{ij}, K_{ijk} .. etc. are the derivatives of the non-linear spring functions and they are defined as

$$
\begin{aligned}
K_{11} &\equiv \frac{\partial N}{\partial \varepsilon} & K_{111} &\equiv \frac{\partial^2 N}{\partial \varepsilon^2} \\
K_{12} &\equiv \frac{\partial N}{\partial \kappa} & K_{112} &\equiv \frac{\partial^2 N}{\partial \varepsilon\, \partial \kappa} \\
K_{21} &\equiv \frac{\partial M}{\partial \varepsilon} & K_{122} &\equiv \frac{\partial^2 N}{\partial \kappa^2} \qquad K_{ij} = K_{ji} \\
K_{22} &\equiv \frac{\partial M}{\partial \kappa} & K_{211} &\equiv \frac{\partial^2 M}{\partial \varepsilon^2} \qquad K_{ijk} = K_{ikj} \\
& & K_{212} &\equiv \frac{\partial^2 M}{\partial \varepsilon\, \partial \kappa} \\
& & K_{222} &\equiv \frac{\partial^2 M}{\partial \kappa^2}
\end{aligned}
\tag{9}
$$

In order to study the postbuckling response of thin-walled columns, and in particular the interaction between local cross-sectional and overall column buckling, the first order instantaneous stiffness coefficients K_{ij} are the most important. They are often called the tangent stiffness coefficients in non-linear structural terminology and they are generally load (state I_s) dependent. Higher order stiffness coefficients are also of interest, but have a less familiar interpretation in structural analysis. They are not discussed in the present report.

For cold formed or welded thin-walled column profiles, initial local imperfections will always be present. The presence of such unavoidable initial imperfections will, even for zero load, give values for the instantaneous stiffness coefficients that deviate from the values that can be achieved for a geometrically perfect column (linear elastic stiffness properties). These initial stiffness values, termed $K_{ij}^{\ 0}, K_{ijk}^{\ 0}, \ldots$, in state I_0, will depend on the size and shape of the local imperfections, which again are strongly related to the material, fabrication and welding procedure used.

The topic of geometrical imperfections and how their magnitude and shape are distributed in real thin-walled stiffened panels are not an issue in this report. Here we assume that the magnitude of the geometrical imperfections is known input parameters, while the imperfection shape is assumed to coincide with the lowest critical eigenmodes. This is a well established and normally conservative assumption.

Assuming that some initial geometrical imperfections exist, the buckling displacements will grow from the very onset of compressive loading, with the consequence that the spring stiffness values gradually decrease. In particular the rate of stiffness degradation will accelerate around the minimum local elastic buckling (local eigenvalues) load.

The present chapter solves and discusses properties of the equilibrium equations under different assumptions with respect to the characteristics of the spring functions, Eq.(6). Section 2.3 solves the problem for compact cross-sections (classical Euler strut) for which Eq.(6) are linear spring functions. Section 2.4 presents a general asymptotic postbuckling solution valid for perfectly straight columns with non-linear spring stiffness properties.

Section 2.5 presents an analytical postbuckling solution valid for perfect straight columns with a bi-linear spring function. A more general numerical solution strategy, applicable for geometrically imperfect thin-walled columns with a general non-linear spring function, is presented in Chapter 3.

2.3 Linear spring stiffness

The simplest case to analyse is the classical case of a compact cross-section and pure linear elastic material behaviour according to Hooke's law ($\bar{\sigma}_x = E\bar{\varepsilon}$). Applying the Bernoulli-Euler assumption, Eq.(4), the stress in a material point in the cross-section is given as

$$\bar{\sigma}_x = E\left[\varepsilon + Z\kappa\right] \tag{10}$$

Substituting Eq.(10) into Eq.(3) gives for the spring forces written on matrix form

$$\begin{bmatrix} N \\ M \end{bmatrix} = \begin{bmatrix} K_{11}{}^{L} & K_{12}{}^{L} \\ K_{21}{}^{L} & K_{22}{}^{L} \end{bmatrix} \begin{bmatrix} \varepsilon \\ \kappa \end{bmatrix} \tag{11}$$

In Eq.(11) the linear stiffness coefficients $K_{ij}{}^{L}$ are defined as

$$\begin{aligned} K_{11}{}^{L} &= EA_T \\ K_{12}{}^{L} &= K_{21}{}^{L} = 0 \quad (12a) \\ K_{22}{}^{L} &= EI_T \end{aligned} \qquad \Rightarrow \text{ giving} \qquad \begin{aligned} N &= (EA_T)\varepsilon \\ M &= (EI_T)\kappa \end{aligned} \tag{12b}$$

In Eq.(12) A_T is the total cross-sectional area, I_T is the moment of inertia of the cross section about the centroid $z = z_G$ and E is Young's modulus. It is noted that $K_{12}{}^{L}$ is zero, which naturally follows from our definition of the reference axis for moment calculation being the centroid of the cross-section. Obviously Eq.(11) is the linear version of Eq.(6).

Substituting Eq.(12) into the equilibrium equations, Eq.(7), and solving for the displacement parameters ε and κ gives

$$\kappa = \frac{P}{P_{Sh} - P}\kappa_0 = \frac{P_{Sh}}{P_{Sh} - P}\kappa_0 - \kappa_0 \tag{13a}$$

$$\varepsilon = P/(EA_T) \tag{13b}$$

In Eq.(13a), P_{Sh} is the Shanley buckling load defined as

$$P_{Sh} = \frac{EI_T}{L\bar{L}} \tag{14}$$

In this report the length $\bar{L}$ of the rigid link is defined as the length giving the same buckling load for the Shanley model as for the classical simply supported continuous Euler column. The classical Euler load P_E is

$$P_E = \frac{\pi^2 EI_T}{L^2} \tag{15}$$

It follows that the present Shanley column length is

$$\bar{L} = \frac{L}{\pi^2} \tag{16}$$

Eq.(13a) represents the classical load-displacement solution for an initially bent beam-column. With reference to the textbook by Croll and Walker (1972) this solution is called the linearized equilibrium path even though it gives a non-linear relation between load P and displacement κ (θ). In other parts of the literature Eq.(13a) is referred to as a second order linearized bending solution. The term $P_{Sh}/(P_{Sh} - P)$ in Eq.(13a) is generally termed amplication factor in the literature. The solution is used in many international codes as basis for strength assessment of beam-columns as well as for stiffened plates and shell structures. As mentioned previously in Section 2.1, application of Eq.(13a) in combination with a first yield approach in an extreme fibre for ultimate capacity assessment, is frequently referred to as the Perry-Robertson approach.

2.4 Initial postbuckling analysis

In order to gain insight into the mechanics of non-linear interactive buckling, and in particular the interaction between local and overall buckling, it is instructive to start with a study of the case of a column with perfect geometry. Perfect means in this context no overall initial deflection of the column axis and no local imperfections in the column cross-section. Koiter (1945) was the first to develop a general theory for the study of the initial postbuckling behaviour of structures with reference to the perfect geometry. His theory can be classified as an asymptotic postbuckling method and a readable introduction can be found in the textbook written by Brush and Almroth (1975) and Dym(1974). In Steen (1989) the Koiter postbuckling parameters for a stiffened panel was derived and compared with a more comprehensive solution based on Marguerre's (1938) plate theory. That model did, however, only include the overall panel buckling mode, neglecting interaction with local modes altogether.

Setting the initial overall imperfection parameter κ_0 equal to zero, the equilibrium equations of the Shanley model, Eq.(7), simplify to

$$\begin{aligned} P - N(\varepsilon, \kappa) &= 0 \\ P\,L\bar{L}\,\kappa - M(\varepsilon, \kappa) &= 0 \end{aligned} \tag{17}$$

Eq.(17) represents two equations in the three unknowns P, ε and κ. Assuming that the postbuckling solution can be expanded around the local critical load level P_C with κ as a continuously increasing parameter, we seek a perturbation solution in the form

$$\begin{aligned} P &= P(\kappa) = P_C + \dot{P}\Delta\kappa + (1/2!)\ddot{P}\,(\Delta\kappa)^2 + \cdots \\ \varepsilon &= \varepsilon(\kappa) = \varepsilon_C + \dot{\varepsilon}\Delta\kappa + (1/2!)\ddot{\varepsilon}\,(\Delta\kappa)^2 + \cdots \end{aligned} \tag{18}$$

Note that in the expansion Eq.(18), the curvature parameter κ is used as the perturbation parameter. A dot over a symbol indicates partial derivative with respect to the curvature parameter κ, and C as subscript indicates state I_C at which initial elastic cross-sectional buckling starts for thin-walled sections. Within the theory of perturbation methods, partial derivatives with respect to some control parameter (here κ) are called path derivatives. It is noted that in the asymptotic power expansion in Eq.(18), the symbol Δκ is used in order to underline that the curvature parameter in general is an incremental property measured from any known state. However, since the power expansion here is measured from a fixed state, corresponding to the perfect straight column state I_C, the incremental symbol Δ could be avoided for convenience of notation.

Substituting the assumed solution, Eq.(18), into the equilibrium equations, Eq.(17), and subsequently carrying out the required differentiation, the following set of incremental equilibrium equations are found.

First order:

$$\begin{aligned} &\dot{P} = \frac{\partial N}{\partial \varepsilon}\dot{\varepsilon} + \frac{\partial N}{\partial \kappa} \\ &\dot{P}L\bar{L}\kappa + PL\bar{L} = \left(\frac{\partial M}{\partial \varepsilon}\dot{\varepsilon} + \frac{\partial M}{\partial \kappa}\right) \end{aligned} \tag{19}$$

Second order:

$$\begin{aligned} &\ddot{P} = \frac{\partial N}{\partial \varepsilon}\ddot{\varepsilon} + \left(\frac{\partial^2 N}{\partial \varepsilon^2}\dot{\varepsilon} + \frac{\partial^2 N}{\partial \varepsilon \partial \kappa}\dot{\kappa}\right)\dot{\varepsilon} + \frac{\partial^2 N}{\partial \varepsilon^2}\dot{\varepsilon} + \frac{\partial^2 N}{\partial \varepsilon \partial \kappa}\dot{\kappa} \\ &\ddot{P}L\bar{L}\kappa + 2\dot{P}L\bar{L} = \frac{\partial M}{\partial \varepsilon}\ddot{\varepsilon} + \left(\frac{\partial^2 M}{\partial \varepsilon^2}\dot{\varepsilon} + \frac{\partial^2 M}{\partial \varepsilon \partial \kappa}\dot{\kappa}\right)\dot{\varepsilon} + \frac{\partial^2 M}{\partial \varepsilon^2}\dot{\varepsilon} + \frac{\partial^2 M}{\partial \varepsilon \partial \kappa}\dot{\kappa} \end{aligned} \tag{20}$$

Higher order solutions can be derived using the same procedure, but are not shown here as they are of secondary interest.

The first order solution is of particular interest as it for thin-walled sections controls the initial phase of the non-linear coupled postbuckling response in the local and overall column mode. Using the definitions for the macro material stiffness coefficients, Eq.(9), and retaining only the first order terms, the solution for $\dot{P}, \dot{\varepsilon}$ around the critical point I_C, i.e. around

$$\begin{aligned} P &= P_C \\ \kappa &= 0 \end{aligned} \tag{21}$$

can be found from Eq.(19) as

$$\dot{P} = \left[\frac{K_{11}}{K_{21}} \left(\frac{P_C}{P_E} (EI_T) - K_{22} \right) + K_{12} \right] \tag{22a}$$

$$\dot{\varepsilon} = \left[\frac{1}{K_{21}} \left(\frac{P_C}{P_E} (EI_T) - K_{22} \right) \right] \tag{22b}$$

Retaining only the first order term in Eq.(18) and inserting the solution from Eq.(22), the final load-curvature relation of the Shanley model, valid in the close neighbourhood of the critical load P_C, is summarised as

$$\Delta P = \left[\frac{K_{11}}{K_{21}} \left(\frac{P_C}{P_E} (EI_T) - K_{22} \right) + K_{12} \right] \Delta\kappa \tag{23a}$$

$$\Delta\varepsilon = \left[\frac{1}{K_{21}} \left(\frac{P_C}{P_E} (EI_T) - K_{22} \right) \right] \Delta\kappa \tag{23b}$$

It is noted that that P_E is the classical Euler load for a simply supported column as defined in Eq.(15). The stiffness coefficients $K_{11}, K_{12} = K_{21}, K_{22}$ are evaluated at state I_C. For thin-walled sections the stiffness coefficients are representative for the integrated cross-sectional behaviour described purely by local buckling modes. Derivations of these stiffness coefficients belong to a separate non-linear postbuckling analysis of thin-walled cross-section and a solution for open stiffener profiles is presented in Chapter 4.

The first order solution presented by Eq.(22), gives a non-zero coefficient $\dot{P}$. According to the Koiter theory this implies that the postbuckling response is asymmetric. The postbuckling parameter $\dot{P}$ can take on both positive and negative values, depending on the relation between the ratio P_C/P_E and cross-sectional stiffness parameters K_{ij}.

As a conclusion, and with reference to Koiter's postbuckling theory, the solution of the initial postbuckling path, Eq.(22), has revealed that the coupling between local and overall buckling mode leads to an initially asymmetric postbuckling behaviour. In other words, as soon as the cross-section of the column starts buckling in some local mode at the load P_C, overall buckling is triggered and the axial load in the column will have to increase or decrease depending on the overall buckling direction. This behaviour is in contrast to a column with a compact cross-section for which a symmetric buckling behaviour will take place at the classical Euler load P_E. It can be mentioned that, within the theory of moderate rotations, the classical compact Euler column has a symmetric neutral postbuckling equilibrium path, which is close approximation up to quite large deflections (elastica).

It is also worth noting that a geometrical perfect column made of inelastic material will buckle (bifurcate) with an initial load increase beyond the tangent modulus load, independent on the overall buckling direction. The reason for this was first pointed out by Shanley (1947) and is attributed to the irreversibility of inelastic material response as opposed to an elastic material response.

Another aspect of the initial postbuckling solution is illuminated when the result is presented in the load-shortening space. This gives possibly the most interesting presentation of the results in relation to a wider application. By considering the column (stiffened panel) as an integrated part of a larger structure, it will be the in-plane load-shortening response (current stiffness) the surrounding structure will sense. Thus load-shortening relations are vital for understanding how load redistribute between gross elements in a large structure.

By eliminating $\Delta\kappa$ between the two equations in Eq.(23) the incremental load-shortening relation is found as

$$\Delta P = S_\varepsilon \Delta\varepsilon \tag{24}$$

where

$$S_\varepsilon = K_{11} + \frac{K_{12}K_{21}}{(P_C/P_E)(EI_T) - K_{22}} \tag{25}$$

The S_ε parameter is the overall in-plane extensional stiffness parameter representing the total effect of both local cross-sectional buckling and overall column buckling. Eq.(25) is discussed in detail in Section 2.5 in connection with the definition of the reduced modulus factor.

It is also of interest to study how the internal moment M at mid-span varies along the initial postbuckling path. Retaining only the first order expansion from Eq.(8), the incremental moment is given as

$$\Delta M = K_{21}\Delta\varepsilon + K_{22}\Delta\kappa \tag{26}$$

By substituting Eq.(23b) into Eq.(26), the axial shortening $\Delta\varepsilon$ is eliminated and the final incremental moment-curvature relation, valid along the postbuckling path, is found as

$$\Delta M = (P_C/P_E)(EI_T)\Delta\kappa \tag{27}$$

Eq.(27) gives an expression for the internal moment acting at the column mid-span, which will counteract the external moment resulting from the axial load P working on a continuously increasing arm (lateral buckling displacement). Since it is assumed here that $P_C < P_E$ always, it follows that the maximum counteracting moment M will occur for a column design with

$$P_C = P_E \tag{28}$$

That the maximum internal moment M is mobilised for a case with $P_C = P_E$ implies the highest degree of instability for such a case. In the language of Koiter's postbuckling theory this means the highest level of asymmetric postbuckling behaviour and the most severe imperfection sensitivity. This is discussed further in Chapter 4.

With a non-zero first order postbuckling coefficient according to Koiter's asymptotic postbuckling theory, we have identified an asymmetric imperfection sensitive column. For small overall initial imperfections (curvature κ_0), the limit buckling load P_M illustrated in Fig.4, can be assessed using Koiter's formula, see e.g. Budiansky and Hutchinson (1979)

$$\frac{P_M}{P_C} \approx 1 - 2(-\dot{P}\,\kappa_0)^{1/2} \tag{29}$$

Fig.4 below illustrates schematically how an asymmetric postbuckling response for a geometrically perfect column (full drawn line) is related to the response of the corresponding geometrically imperfect column (dotted lines). The maximum limit buckling load P_M will be lower than the buckling load P_C, and the degree of knock down due to geometrical imperfections follows Koiter's asymptotic formula exactly for very small imperfection levels. In other words, the Koiter formula calculates directly the buckling capacity P_M for a geometrical imperfect column knowing the value of the postbuckling parameter $\dot{P}$. (Instead of $\dot{P}$ the symbol a_1 is frequently used in the literature for the first order postbuckling coefficient and a_2 for the second order coefficient, see e.g. Brush and Almroth (1975), Steen (1989)).

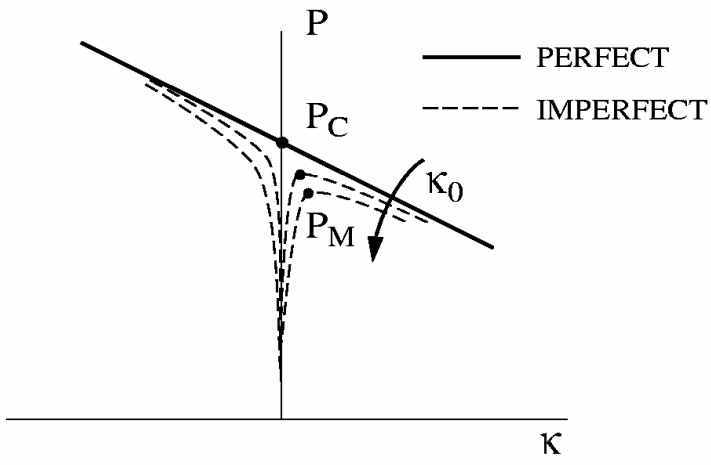

Fig.4. Load-buckling deflection response for asymmetric buckling

2.5 Analytical postbuckling solution for geometrically perfect columns

It is of interest to derive a general analytical postbuckling solution, which is valid not only in the initial postbuckling region as the Koiter theory, but also in the advanced postbuckling region. In order to derive such a solution some assumptions have to be made as discussed briefly in the following.

The asymptotic postbuckling solution as presented in Section 2.4, assumed the stiffness coefficients K_{ij} to be evaluated at the local critical buckling load P_C (state I_C). Moving along the postbuckling path, branching off at P_C, the values for the K_{ij} coefficients would normally change from the values at P_C. In order to cope with this effect, involving a continuously updating of the current stiffness coefficients, a numerical solution technique will be needed. However, it has for a long time been recognised that the local stiffness coefficients for thin-walled built up sections in many cases can be considered as having fixed values, valid well into the advanced postbuckling region. Such fixed postbuckling characteristics of plate elements are confirmed by the analysis presented in Chapter 4 and Chapter 5 in this report. See e.g. Rhodes(1982) for a useful review of postbuckling solutions of plates.

By adopting the assumption of fixed postbuckling stiffness coefficients K_{ij} (with values as evaluated at P_C), an analytical solution for the advanced postbuckling region is presented in the following. The derivations are based on the equilibrium equation for a geometrically perfect Shanley column, Eq.(17), and by specifying a bi-linear characteristic for the macro model.

When assuming the first order stiffness coefficients K_{ij} to be fixed and not varying along the postbuckling path, the higher coefficients K_{ijk} ..etc. are zero. It then follows from Eq.(8) that the incremental bi-linear spring law for the postbuckling path is given as

$$\begin{aligned} \Delta N &= K_{11}\Delta\varepsilon + K_{12}\Delta\kappa \\ \Delta M &= K_{21}\Delta\varepsilon + K_{22}\Delta\kappa \end{aligned} \qquad K_{12} = K_{21} \tag{30}$$

For the case of a geometrically perfect column it follows that at the point of local cross-sectional buckling, the cross-sectional axial load N_C and moment M_C are

$$\begin{aligned} N_C &= P_C \\ M_C &= 0 \end{aligned} \tag{31}$$

Using Eq.(30) and Eq.(31) the general non-linear spring law, Eq.(6), takes the form

$$\begin{aligned} N(\varepsilon,\kappa) &= P_C + K_{11}\varepsilon + K_{12}\kappa \\ M(\varepsilon,\kappa) &= K_{12}\varepsilon + K_{22}\kappa \end{aligned} \tag{32}$$

Note that symbol Δ has been avoided in Eq.(32) for the incremental strain ε and curvature κ for convenience of notation. Substituting Eq.(32) into the equilibrium equation, Eq.(17), and rearranging gives the analytical load-curvature relation

$$\frac{P}{P_R} = \frac{\frac{P_C}{P_R} - \frac{K_{11}}{K_{12}}\frac{EI_T}{P_E}\kappa}{1 - \frac{K_{11}}{K_{12}}\frac{EI_T}{P_E}\kappa} \tag{33}$$

In Eq.(33) P_R is the *reduced modulus buckling load* defined as

$$P_R = (K_{22} - \frac{K_{12}K_{21}}{K_{11}})/(L\bar{L}) \tag{34}$$

As mentioned in Section 2.2 the present general description of the Shanley spring model do not explicitly consider the physical reason for the stiffness coefficients K_{ij}, i.e. it can be either due to a purely non-linear elastic material effect or due to a non-linear geometrical effect. However, for the solution Eq.(33) to be valid the K_{ij} coefficients must be constants along the postbuckling path. Since this is a typical feature for local postbuckling behaviour of thin-walled sections, it is natural to have this type of response as a reference when discussing the solution, Eq.(33).

When analysing Eq.(33) it is useful to be aware of the physical implication of the different parameters. For a thin walled cross-section the K_{11} coefficient represents the axial stiffness after local buckling, and it will always be a positive number. The coefficient K_{22} represents the bending stiffness about the centroid of the section, and it will also always be a positive number. The coupling term K_{12} (= K_{21}) represent the shift in neutral axis due to local cross-sectional buckling. It is negative if the cross-sectional buckling involves a shift in neutral axis along the positive z-axis and positive in the opposite case. This sign convention for K_{12} is accompanied with a positive value of the lateral curvature parameter κ when the column buckles in the direction of the positive z-axis.

Another parameter entering the analytical postbuckling solution in Eq.(33), is the *reduced modulus buckling load* P_R. Since the reduced modulus load for quite some time has been recognised as an important concept in the elastic interactive postbuckling theory, and since it emerge in the analytical postbuckling solution as parameter, some space are used in the following to give a description of its main features.

The reduced modulus load in the elastic interactive buckling theory is defined as the buckling load for which the coupled local and overall buckling response will progress along a neutral equilibrium path (see e.g. Walker (1975) or Croll and Walker (1972)). This implies that there is no incremental load increase (or drop) ΔP along the postbuckling path. Mathematically this is expressed as

$$\Delta P = 0 \tag{35}$$

It is seen from Eq.(24) that Eq.(35) is the same as requiering

$$S_\varepsilon = 0 \tag{36}$$

Rearranging Eq.(36), using Eq.(25), gives the condition for a neutral equilibrium path as

$$\frac{P_C}{P_E}(EI_T) = K_{22} - \frac{K_{12}K_{21}}{K_{11}} \tag{37}$$

In Section 2.4 a general expression for the moment-curvature relationship valid along any postbuckling path was found in the form of Eq.(27). Substituting Eq.(37) into Eq.(27) gives the moment-curvature relationship valid along the coupled neutral equilibrium path as

$$\Delta M = (K_{22} - \frac{K_{12}K_{21}}{K_{11}})\Delta\kappa \tag{38}$$

Comparing Eq.(38) and the corresponding moment-curvature relationship for a compact cross-section, Eq.(12b) it is natural to define a relative bending stiffness parameter. In the literature dealing with elastic interactive buckling this parameter has been called *the reduced modulus factor*, symbolised here as η_{BR}. It follows from Eq.(38) and Eq.(12b) that it is mathematically defined as

$$\Delta M = \eta_{BR}(EI_T)\Delta\kappa \tag{39}$$

where per definition

$$\eta_{BR} = (K_{22} - \frac{K_{12}K_{21}}{K_{11}})/(EI_T) \tag{40}$$

B as a subscript indicates bending and R for reduced modulus, respectively.

Substituting Eq.(40) into Eq.(34) gives the final compact expression for the reduced modulus load as

$$P_R = \eta_{BR}(EI_T)/(L\bar{L}) \tag{41}$$

Eq.(41) is similar to Eq.(14) describing the buckling load of the Shanley column, but with the reduced bending stiffness of the column instead of the full bending stiffness.

The properties of the analytical postbuckling solution Eq.(33), with reference to Fig. 5 for a schematic illustration, are briefly summarised as follows

i) If $K_{12} < 0$ and $P_C > P_R$, the postbuckling path is descending for positive curvature κ and it converges towards the reduced modulus load P_R as the lower bound value. The most descending postbuckling path is identified for $P_C = P_E$ which indicates the most severe imperfection sensitivity for coincident buckling in the local and overall mode. Conclusion: *unstable postbuckling response*.

ii) If $K_{12} < 0$ and $P_C < P_R$, the postbuckling path is rising above the initial buckling load P_C, approaching P_R as the upper limit value. Conclusion: *stable postbuckling response*.

iii) If $P_C > P_E$ the column will buckle in the Euler mode first and local buckling will be initiated subsequently with P descending along the secondary postbuckling path.

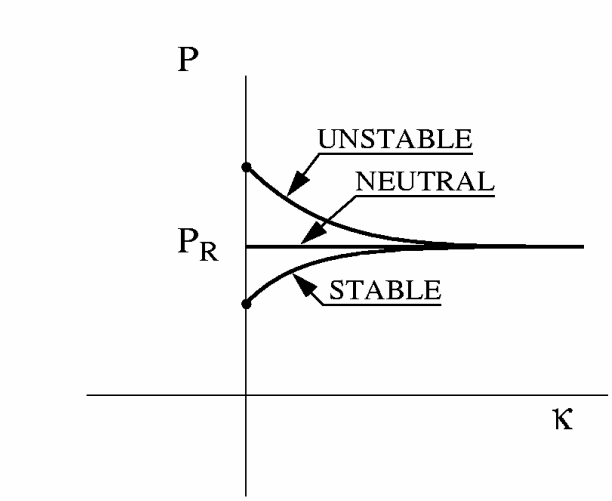

Fig.5. Load- curvature (rotation) curves for the geometrically perfect Shanley model, schematically

As mentioned in Section 2.4 it is also important to discuss the postbuckling response of the coupled local and overall mode in a load-shortening visualisation. For simplicity we use the expression for the expanded postbuckling stiffness S_ε (around P_C), Eq. (25). By introducing the reduced modulus load P_R, i.e. substituting Eq.(34) into Eq.(25), the axial stiffness parameter is rewritten as

$$S_\varepsilon = \frac{P_C - P_R}{\frac{1}{K_{11}}(P_C - P_E \frac{K_{22}}{EI_T})} \qquad (42)$$

It is remarked that the axial stiffness as expressed by Eq.(42) includes both the local and overall buckling modes in interaction. Eq.(42) reveals interesting features, which are illustrated schematically in Fig. 6.

As seen from Eq.(42) the S_ε coefficient may take both positive and negative values. The actual value depends on the ratios between the stiffness coefficients K_{ij}, the local buckling load P_C and the overall Euler buckling load P_E.

A positive value for S_ε larger than full linear stiffness value EA_T indicates snap back buckling, i.e. the shortening ε has to decrease in order to follow the equilibrium path beyond the initial buckling load P_C. If the following two conditions are satisfied, i.e. if

$$P_C = P_E$$
$$\frac{P_R}{P_C} = 1 - (1 - \frac{K_{22}}{EI_T})\frac{EA_T}{K_{11}} \qquad (43)$$

the maximum degree of snap back, i.e. $S_\varepsilon = EA_T$ occurs.

A positive value for S_ε less than EA_T indicates a stable postbuckling response with a rising equilibrium path beyond P_C. Moreover a value for S_ε equal to zero means neutral stability. From Eq.(42) it is seen as that this will be the case if $P_C = P_R$. A negative value for S_ε represents an unstable postbuckling behaviour with a descending load P accompanied with an increase in shortening ε.

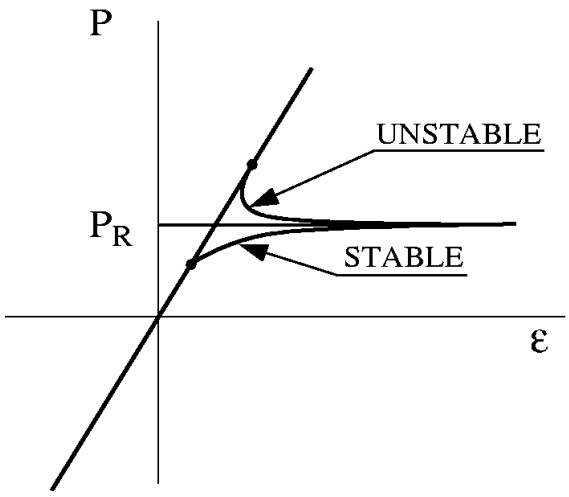

Fig.6 Load-shortening curves for the geometrically perfect Shanley model, schematically

A major feature of the present analytical postbuckling solution is that it approaches the reduced modulus load P_R in the advanced postbuckling region. Thus by using the reduced modulus load as the lower limit for the buckling strength, unstable postbuckling behaviour and imperfection sensitivity is eliminated. However, this will be a very conservative approach and alternative methods have to be preferred. One alternative will be to use a comprehensive numerical procedure tracing the full non-linear equilibrium path as described in Chapter 3.

2.6 Summary and discussion

In this chapter the mechanics involved in the non-linear elastic interactive buckling of columns has been explored from an overall point of view. A two-dimensional macro model has been introduced for the purpose of describing the integrated effect of the non-linear cross-sectional response.

A Shanley model has been used for coupling the macro model to the overall buckling response of the column. Closed form solutions for the coupled postbuckling response has been derived using a perturbation expansion approach according to Koiter's method. Closed formed solution for the advanced postbuckling equilibrium path has been found valid under the condition of constant postbuckling stiffness coefficients. The advanced postbuckling solution verifies that the reduced modulus load gives a conservative assessment of the buckling load by completely eliminating the unstable interaction between local and overall buckling.

For thin-walled sections the macro material model is a compact way of formulating the local cross-sectional buckling response, including the non-linear geometrical effect and linear elastic material law (Hooke's law). This is explained in more depth in Chapter 3 for macro material models for thin-walled cross-sections.

The description in this chapter is rather general and does not specifically address the problem of buckling of thin-walled cross-sections. However, most of the assumptions implemented and special solutions presented are typical for thin-walled sections.

3. THE SHANLEY MODEL FOR THIN-WALLED CROSS SECTIONS

3.1 General section macro material formulation

In Chapter 2 the two-dimensional *macro model* was assumed to have the general closed form as given by Eq.(6). This form does not reveal the origin for the non-linearity, i.e. whether it is due to a material or geometrical effect. In the present chapter, dealing with local buckling of thin-walled built up sections, the non-linearity will be linked exclusively to the local geometrical effect. This is done mathematically by introducing the K-dimensional displacement vector q_i, describing all relevant buckling modes in the cross-section. The *macro model* can then be written as functions of the displacement control parameter ε and κ in addition to the q_i.

For any component plate in the cross-section the total membrane stress in the x-direction can generally be written on the form

$$\overline{\sigma}_x = \overline{\sigma}_x(\varepsilon, \kappa, q_i) \qquad i = 1,2,\ldots,K \qquad (44)$$

It will be shown in Chapter 4 that functions in the form of Eq.(44) can be written as the sum of a linear part and a non-linear part. According to classical buckling theory these two parts are the direct applied stresses (prebuckling solution) and secondary stresses (postbuckling solution) due to the buckling displacments q_i, respectively.

By substituting Eq.(44) into Eq.(3) and carrying out the integrations, the total cross-sectional loads can be written in matrix notation as

$$\begin{bmatrix} N \\ M \end{bmatrix} = \begin{bmatrix} K_{11}{}^{L} & K_{12}{}^{L} \\ K_{21}{}^{L} & K_{22}{}^{L} \end{bmatrix} \begin{bmatrix} \varepsilon \\ \kappa \end{bmatrix} + \begin{bmatrix} g_N(q_i) \\ g_M(q_i) \end{bmatrix} \qquad i = 1,2,\ldots,K \qquad (45)$$

In Eq.(45) the first term represents the linear contribution and the second part represents the non-linear geometrical contribution through the functions $g_N(q_i), g_M(q_i)$. The latter functions can be derived analytically for a simple two-degree of freedom model, as shown in Chapter 4.

For compactness of notation, Eq.(45) can be written as

$$\begin{aligned} N &= N(\varepsilon, \kappa, q_i) \\ M &= M(\varepsilon, \kappa, q_i) \end{aligned} \qquad i = 1,2,\ldots,K \qquad (46)$$

In the language of perturbation methods a displacement control case in space (ε, κ) requires a solution in the form

$$q_i = q_i(\varepsilon, \kappa) \qquad i = 1,2,\ldots,K \qquad (47)$$

of the K local equilibrium equations

$$f_i(\varepsilon, \kappa, q_i) = 0 \qquad i = 1,2,\ldots,K \qquad (48)$$

Note that the q_i is used as symbols for the functions as well as for the displacement parameters, despite the lack of mathematical rigor this notation represents. It is also mentioned that it is not always possible to achieve single valued solutions in the form of Eq.(47), and it may be necessary to resort to the more general multiple dimensional arc length approach, Steen(1998). This is not discussed further here since for the model in Chapter 4 solutions in the form of Eq.(47) are available.

By substituting the solution Eq.(47) into Eq.(45), the q_i parameters are eliminated, and the macro material relations take the general form

$$\begin{bmatrix} N \\ M \end{bmatrix} = \begin{bmatrix} K_{11}{}^{L} & K_{12}{}^{L} \\ K_{21}{}^{L} & K_{22}{}^{L} \end{bmatrix} \begin{bmatrix} \varepsilon \\ \kappa \end{bmatrix} + \begin{bmatrix} g_N(q_i(\varepsilon, \kappa)) \\ g_M(q_i(\varepsilon, \kappa)) \end{bmatrix} \qquad i = 1,2,\ldots,K \qquad (49)$$

Eq.(49) is from an overall point of the view the same as the macro model, Eq.(6), i.e. the displacement parameters q_i are hidden. Thus it could equally represent a non-linear elastic material, say of rubber, or represent a deformation theory of plasticity. This is the motivation for calling this format a *macro material* formulation.

It follows from Eq.(9) and Eq.(49) that the first order stiffness coefficients are given as

$$
\begin{aligned}
K_{11} &= K_{11}^{\,L} + \frac{\partial g_N}{\partial q_i}\frac{\partial q_i}{\partial \varepsilon} \\
K_{12} &= K_{12}^{\,L} + \frac{\partial g_N}{\partial q_i}\frac{\partial q_i}{\partial \kappa} \\
K_{21} &= K_{21}^{\,L} + \frac{\partial g_M}{\partial q_i}\frac{\partial q_i}{\partial \varepsilon} \\
K_{22} &= K_{22}^{\,L} + \frac{\partial g_M}{\partial q_i}\frac{\partial q_i}{\partial \kappa}
\end{aligned}
\qquad i = 1,2,\ldots,K \qquad (50)
$$

Knowing the analytical expressions for the $g_N(q_i)$ and $g_M(q_i)$ functions, the partial derivatives $\partial q_N / \partial q_i$, $\partial q_M / \partial q_i$ are directly available (see Chapter4).

The unit directional path derivatives $\partial q_i / \partial \varepsilon$, $\partial q_i / \partial \kappa$ can be found by solving the corresponding equilibrium equations. Substituting Eq.(47) into Eq. (48) and taking the partial derivatives with respect to ε and κ, gives two set of equations for finding the unit directional path derivatives, i.e. we have

$$
\begin{aligned}
\frac{\partial f_i}{\partial q_j}\frac{\partial q_j}{\partial \varepsilon} + \frac{\partial f_i}{\partial \varepsilon} &= 0 \\
\frac{\partial f_i}{\partial q_j}\frac{\partial q_j}{\partial \kappa} + \frac{\partial f_i}{\partial \kappa} &= 0
\end{aligned}
\qquad i, j = 1,2,\ldots,K \qquad (51)
$$

The purpose of the present derivation was to demonstrate that the perturbation procedure gives a method for explicit assessment of the current macro material coefficients K_{11}, K_{12}, K_{22}. In a wider range of application this feature can be utilised for stiffness assessment of buckled panels subjected to combined loads, which again can be utilised in FE models for ship hull redundancy assessment. This explicit approach is used in Chapter 4 and Chapter 5 for open thin-walled cross-section.

In the next section, the macro model in the form of Eq.(46) is used together with the global equilibrium equations, Eq.(7), to formulate the interactive global and local cross-sectional buckling problem of an axially loaded column.

3.2 Numerical solution method - Imperfect geometry

For the case of a column with imperfect geometry both in the form of axial out-of-straightness of the column axis (a non-zero κ_0) and out-of-flatness of the component plates in the cross-section (a non-zero initial displacement vector q_{i0}), it is not possible to derive closed form equilibrium solutions. Thus resort to a numerical scheme is necessary. For this purpose,

the perturbation procedure used in an incremental scheme, as described in detail by Steen (1998), have been adopted.

According to the author's knowledge, the perturbation method used in an incremental scheme for solving structural stability problems is a rather unexplored field. However, since the perturbation method is a novel and accepted approach in stability theory, it is natural to extend its application for tracing non-linear continuous equilibrium paths. The present numerical scheme applies such a strategy by stepping along the equilibrium path from zero loads in small increments. A brief description of the method is given in the following while Chapter 5 presents two specific examples.

The basis for the numerical model is the analytical macro material model in the form of Eq.(46). Assuming that such a set of algebraic equations exists, we substitute Eq.(46) into the equilibrium equations, Eq.(7). This gives two non-linear algebraic equilibrium equations in the 3 + K unknowns (P, κ, ε, q_i) as follows

$$\begin{aligned} P &= N(\varepsilon, \kappa, q_i) \\ P\,L\bar{L}\,(\kappa + \kappa_0) &= M(\varepsilon, \kappa, q_i) \end{aligned} \tag{52}$$

In addition to these global equilibrium equations it is assumed that there exist K local equilibrium equations. For the sake of completeness these K local equilibrium equations, Eq.(48), are repeated as

$$f_i(\varepsilon, \kappa, q_i) = 0 \qquad (i = 1,2,\ldots,K) \tag{53}$$

In total this gives 3 + K unknowns and 2 + K equations. In a perturbation solution strategy it is necessary to choose a control parameter with the property of being continuously increasing along the equilibrium path. For the present single load (axial load) column buckling problem, the curvature parameter κ will for most cases be such a parameter. However, as shown by the analytical solution in Section 2.5, snap back problems may exist for special geometrical proportions, with subsequent decrease of the κ parameter. Thus it generally cannot be assumed that κ is a continuously increasing parameter and the more generalised concept of the arc length parameter, symbolised by η, is a more proper choice. This is more thoroughly discussed in Steen(1998) and applied in the following.

The arc length perturbation parameter η is defined as

$$\eta - \eta_s = \dot{q}_i(q_i - q_i^{\,s}) + \dot{\varepsilon}(\varepsilon - \varepsilon_s) + \dot{\kappa}(\kappa - \kappa_s) + \dot{P}(P - P_s) \tag{54}$$

Eqs.(52),(53) and Eq.(54) constitutes the necessary 3+K equations in the 3+K unknowns and the perturbation solution can now be written as

$$
\begin{aligned}
P &= P_{,s} + \dot{P}(\eta - \eta_s) + (1/2!)\ddot{P}(\eta - \eta_s)^2 + \cdots \\
\varepsilon &= \varepsilon_{,s} + \dot{\varepsilon}(\eta - \eta_s) + (1/2!)\ddot{\varepsilon}(\eta - \eta_s)^2 + \cdots \\
\kappa &= \kappa_{,s} + \dot{\kappa}(\eta - \eta_s) + (1/2!)\ddot{\kappa}(\eta - \eta_s)^2 + \cdots \\
q_1 &= q_{1,s} + \dot{q}_1(\eta - \eta_s) + (1/2!)\ddot{q}_1(\eta - \eta_s)^2 + \cdots \\
q_2 &= q_{2,s} + \dot{q}_2(\eta - \eta_s) + (1/2!)\ddot{q}_2(\eta - \eta_s)^2 + \cdots \\
&\vdots
\end{aligned}
\qquad (55)
$$

Thus by knowing one equilibrium state I_s and the associated first, second (and possibly higher order) path derivatives, the next state I_{s+1} can be found directly by stepping along the equilibrium path using small values of the incremental perturbation parameter $\Delta\eta = \eta - \eta_s$. It is noted that the present arc length concept requires the solution space (P, κ, ε, q_i) to be scaled such that all parameters are without dimensions. As small s as super or subscript indicates a known value in state I_s.

The selected size of the incremental perturbation parameter $\Delta\eta$ and the number of terms in the power expansion are not a critical issue in this report, since very simple models with few degrees of freedoms are used. Naturally, for larger problems with many degrees of freedom, the problem of computer time and solution efficiency will be an important issue, but as said this topic is not discussed in this report.

3.3 Summary

This chapter presented the concept of a local macro material formulation for thin-walled built up sections, introducing the buckling displacement vector q_i to describe all relevant local buckling modes in a cross-section. Within the perturbation methodology, an explicit form for the current macro stiffness coefficients is developed. Moreover, a brief description of an incremental perturbation scheme for tracing non-linear continuous equilibrium paths for geometrically imperfect columns is given. The arc length along the equilibrium path is chosen as the independent perturbation (control) parameter, a choice which enables the procedure to pass limit points and snap-back problems as illustrated by examples in Chapter 5.

4. MACRO MODEL FOR OPEN STIFFENER PROFILES

4.1 General

As introduced in Section 2.1, the integrated non-linear geometrical response of a column cross-section can be treated as a pseudo material formulation, here called a *macro material model*. In the linear terminology, the macro material concept is well established and synonymous with a general section shell element, in which the stiffness properties in all

directions can be specified. This is a type of element formulation that is provided in several modern general purpose finite element codes, e.g. in ABAQUS(1996).

For describing the non-linear response, the method of including the local cross-sectional buckling response as a pseudo material, was first introduced by Smith (1975). His method was based on isolation and pre-calculation of the local plate buckling response, generating the in-plane average stress-strain behaviour of the plate flange. The local buckling amplitudes (present q_i vector) was not seen in the procedure. Based on the calculated average stress-strain behaviour of the attached plate flange, a general Newton-Raphson type of solution technique was used for calculating the interactive column buckling response. This method constituted a very interesting approach for simplified buckling analysis of panels with solid stiffeners and thin plating, but lacked the generality needed for dealing other types of local stiffener failure modes.

The present concept of a macro material model embeds all types of cross-sectional buckling modes into the same pseudo spring law formulation. As an example of a specific macro model, a simplified formulation for open stiffener profiles attached to continuous plates, typical for panel designs in ship and offshore structures has been developed in this chapter. With respect to relevant buckling modes this means that torsional stiffener buckling as well as stiffener web buckling, interacting with local buckling of the continuous plate, are considered.

As a general introduction to the present *macro modelling* technique, the six-dimensional formulation of a stiffened panel as illustrated in Fig.7, is briefly discussed. Later the two-dimensional *macro* formulation sufficient for coping with uni-axially loaded panels is dealt with in more detail.

Stiffened panels are built up from thin-walled *component plates* with certain boundary conditions along their junction lines. Integration of the membrane stresses across a panel unit section according to a six-dimensional generalisation of Eq.(3), will give for the non-linear *macro material law*, relations in the form

$$\begin{aligned}
N_1 &= N_1(\varepsilon_1,\varepsilon_2,\varepsilon_3,\kappa_1,\kappa_2,\kappa_3)\\
N_2 &= N_2(\varepsilon_1,\varepsilon_2,\varepsilon_3,\kappa_1,\kappa_2,\kappa_3)\\
N_3 &= N_3(\varepsilon_1,\varepsilon_2,\varepsilon_3,\kappa_1,\kappa_2,\kappa_3)\\
M_1 &= M_1(\varepsilon_1,\varepsilon_2,\varepsilon_3,\kappa_1,\kappa_2,\kappa_3)\\
M_2 &= M_2(\varepsilon_1,\varepsilon_2,\varepsilon_3,\kappa_1,\kappa_2,\kappa_3)\\
M_3 &= M_3(\varepsilon_1,\varepsilon_2,\varepsilon_3,\kappa_1,\kappa_2,\kappa_3)
\end{aligned} \qquad (56)$$

In this six-dimensional form, it is most convenient to use subscript 1 for the force in x_1 direction, subscript 2 for a force in the x_2 direction and subscript 3 for the shear force in the x_1-x_2 plane. The same notation applies for the bending moments acting out-of-plane and for the corresponding average reference strains and curvatures. By expanding this six-dimensional *macro material law*, as done principally for the two-dimensional spring in Eq. (8), and retaining only the first order terms, the *incremental macro material law* can be written as

$$\begin{bmatrix} \Delta N_1 \\ \Delta N_2 \\ \Delta N_3 \\ \Delta M_1 \\ \Delta M_2 \\ \Delta M_3 \end{bmatrix} = \begin{bmatrix} C_{11} & C_{12} & C_{13} & Q_{11} & Q_{12} & Q_{13} \\ C_{21} & C_{22} & C_{23} & Q_{21} & Q_{22} & Q_{23} \\ C_{31} & C_{32} & C_{33} & Q_{31} & Q_{32} & Q_{33} \\ Q_{11} & Q_{21} & Q_{31} & D_{11} & D_{12} & D_{13} \\ Q_{12} & Q_{22} & Q_{32} & D_{21} & D_{22} & D_{23} \\ Q_{13} & Q_{23} & Q_{33} & D_{31} & D_{32} & D_{33} \end{bmatrix} \begin{bmatrix} \Delta\varepsilon_1 \\ \Delta\varepsilon_2 \\ \Delta\varepsilon_3 \\ \Delta\kappa_1 \\ \Delta\kappa_2 \\ \Delta\kappa_3 \end{bmatrix} \qquad (57)$$

In Eq.(57) the C_{ij} coefficients symbolise the in-plane stiffness properties, the D_{ij} coefficients symbolise the out-of plane bending stiffness properties and the Q_{ij} coefficients symbolise the coupling between in-plane and out-of -plane action. The latter coupling is typical for eccentrically stiffened panels, Fig.7, which represent the usual design in ship and offshore structures.

It is noted that the twisting moment per unit length for an orthotropic panel unit will be different in the two orthogonal directions, i.e. M_3' is different from M_3'', Fig.7. In the stiffness relation, Eq.(57), the average sum $M_3 = (M_3' + M_3'')/2$ is given. Due to the strict matrix convention for stiffness coefficients used here, the twisting coefficient D_{33} is twice of what is often seen in the literature. (In Timoshenko and Woinowsky-Krieger (1959) D_{xy} symbolise the twisting coefficient, i.e. $D_{33} = 2D_{xy}$. In Smith(1990) D_{66} symbolise the twisting coefficient, i.e. $D_{33} = 2D_{66}$. In the finite element code ABAQUS (1996) D_{33}^{ABAQUS} symbolise the twisting coefficient, i.e. $D_{33} = 2D_{33}^{ABAQUS}$)

In the present work, the standard text book strain measures are used, see e.g. Brush and Almroth (1975). Thus it should be noted that the shear strain ε_3 in Eq.(57) is twice the classical shear strain (i.e. $\varepsilon_3 = 2\varepsilon_{12}$ where ε_{12} is the classical strain tensor component). The curvature measures are according to the classical definitions $\kappa_1 = - w_{,11}$, $\kappa_2 = - w_{,22}$, $\kappa_3 = - w_{,12}$ where w symbolise the plate deflection normal to the reference surface and a subscript 1 represent partial differentiation with respect to co-ordinate x_1 etc. (In ABAQUS(1996) the engineering strain measurements are used, i.e. our κ_3 is $(½)\kappa_{12}^{ABAQUS}$ which explains that D_{33} is 2 times D_{33}^{ABAQUS}).

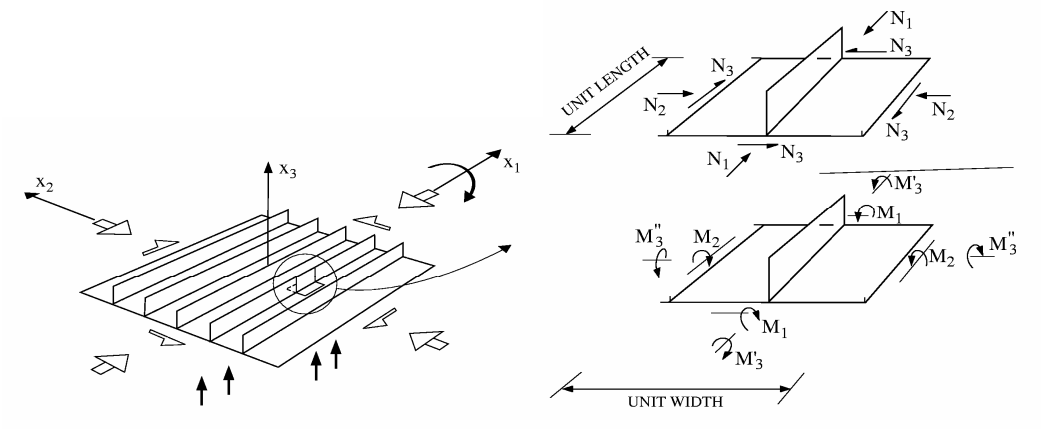

Fig. 7 Six-dimensional macro model for stiffened panels

The six-dimensional macro material model is not pursued further in this report since a two-dimensional representation is sufficient for the study of elastic overall buckling of a uni-axially loaded column.

The rest of this chapter is exclusively devoted to the development of a two-dimensional *macro material law* for an open thin-walled profile attached to continuous thin plating. The open stiffener profile is attached to the plating with a regular spacing s and the geometrical layout is as illustrated in Fig.8.

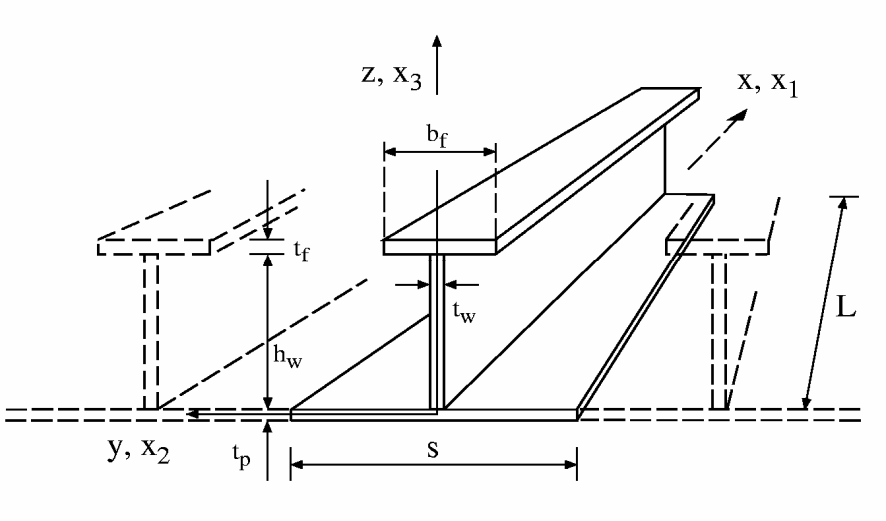

Fig.8 Geometry of stiffened panel with open T stiffener profile

The two-dimensional *macro model* assumes that the continuous plating is free to deform in the x_2 direction due loading in the x_1 direction. Likewise the stiffener web plate is free to expand in the x_3 direction when compressed in the x_1 direction. The stiffener flange is considered to be a beam element. These assumptions provide for a pure uni-axial nominal stress condition for all component plates in the panel.

For convenience of notation the subscript 1 for the axial load and moment respectively (and strains ε_1 and κ_1), is not needed for the present two-dimensional problem and is consequently not used in the rest of this chapter.

In Chapter 2, Eq.(9), the first order stiffness coefficients were symbolised as K_{ij}. This has been done to avoid confusion with the more general six-dimensional description. In particular C_{11} is not equal to K_{11}, D_{11} is not equal to K_{22}, etc. This follows from the assumption of free transverse displacements of the continuous plating in the x_2-direction and the location of the reference plane. For the six-dimensional model it will be most convenient to use the continuous plating as the reference plane. In the present two-dimensional model it is most convenient to use the centroid of the cross-section, since this gives decoupled bending and membrane behaviour in the linear elastic range, i.e. $K_{12} = 0$ if buckling is excluded.

For the sake of brevity, Marguerre's non-linear plate theory is summarised in the following section. This theory has been used for developing the two-dimensional macro model. Both the continuous plating and the web stiffener plate have been considered as individual component plates using this thin-walled plate theory, while the stiffener flange has been treated as a beam.

4.2 Marguerre's non-linear plate theory

Marguerre (1938) developed a shallow non-linear plate theory, accounting for out-of-flatness from perfect form. His theory has been extensively used in the literature for the study of plate buckling problems. The theory belongs to the category of non-linear small strain approximation and is valid for moderately large deflections, see Brush and Almroth (1975). For geometrically perfect plates it resembles the classical von Karman plate theory, see Washizu (1975) for a full account of the theory. In this section standard tensor notation is used when found convenient.

For illustration, Marguerre's basic equations are summarised with reference to a single plate with geometry as shown in Fig.9.

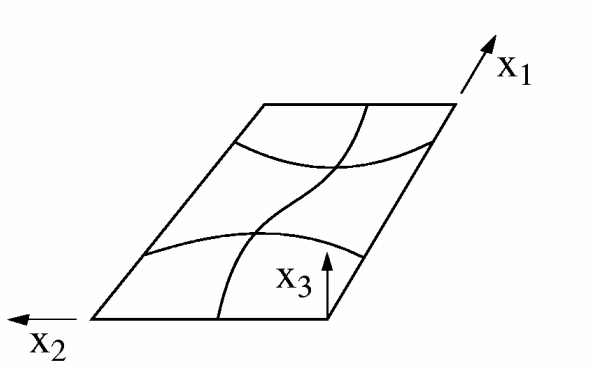

Fig.9. Component plate as part of a stiffened panel

Marguerre's plate theory applies the classical displacement hypothesis of Love-Kirchhoff, i.e. the displacements $(\bar{u}_\alpha, \bar{w})$ of any point outside the reference plane is related to the displacements (u_α, w) of the reference plane as

$$\begin{aligned} \bar{u}_\alpha &= u_\alpha - x_3 w_{,\alpha} \\ \bar{w} &= w \end{aligned} \qquad \alpha, \beta = 1,2 \qquad (58)$$

A bar over the parameter signifies evaluation at any material point in the plate. A Greek letter followed by a comma indicates partial derivative with respect to the corresponding rectangular x_α co-ordinate. Parameters without a bar signify evaluation at the reference

surface, which is taken to be the plate's middle plane. The u_α symbolise the in-plane displacement in the x_α direction, while w symbolise the displacement normal to the plate plane, i.e. in the x_3 direction.

From the Love-Kirchhoff thin-shell approximations it follows that

$$\bar{\varepsilon}_{\alpha\beta} = \varepsilon_{\alpha\beta} - x_3\kappa_{\alpha\beta} \qquad \alpha, \beta = 1,2 \qquad (59)$$

The plate middle plane curvature $\kappa_{\alpha\beta}$ is defined as

$$\kappa_{\alpha\beta} = -w_{,\alpha\beta} \qquad \alpha, \beta = 1,2 \qquad (60)$$

The membrane strain tensor $\varepsilon_{\alpha\beta}$ of the middle plate plane are according to Marguerre's plate theory defined as

$$\varepsilon_{\alpha\beta} = \frac{1}{2}(u_{\alpha,\beta} + u_{\beta,\alpha} + w_{0,\alpha}w_{,\beta} + w_{0,\beta}w_{,\alpha} + w_{,\alpha}w_{,\beta}) \qquad \alpha, \beta = 1,2 \qquad (61)$$

The w_0 is the stress free initial out-of-flatness of the reference surface and u_1 and u_2 are the in-plane displacement in the x_1 and x_2 direction respectively due to applied loading.

Marguerre's compatibility equation is given as

$$\nabla^4 F = E\left[(w + w_0)_{,12}^2 - (w + w_0)_{,11}(w + w_0)_{,22} - (w_{0,12}^2 - w_{0,11}w_{0,22})\right] \qquad (62)$$

where the F is Airy's stress function defined as

$$\begin{aligned} \sigma_{11} &= F_{,22} \\ \sigma_{22} &= F_{,11} \\ \sigma_{12} &= -F_{,12} \end{aligned} \qquad (63)$$

and σ_{11}, σ_{22}, σ_{12} are the membrane stresses in the plate according to standard tensor notation.

In the following sections this non-linear plate theory is used for formulating the local buckling and postbuckling problem of stiffened panels with open stiffener profiles.

4.3 Local buckling of an open profile cross-section

4.3.1 General

The present two-dimensional *macro model* is developed for a stiffened panel with geometry as shown in Fig.8. Note that, the rectangular Cartesian system (x, y, z) is used instead of (x_1, x_2, x_3) in the present two-dimensional formulation.

The cross-section is assumed to buckle into two different local modes as classified in Section 4.3.2. This implies that both the continuous plating and stiffener web plate are allowed to buckle locally, while the stiffener flange may twist and bend without changing cross-sectional shape.

The most important assumption in the present classification of local buckling modes is that the junction line between the continuous plating and stiffener web plate are constrained to be in the plate plane (x,y). The background for this assumption needs some comments.

In the present model the stiffener web plate is considered to be a component plate with no constraint in z-direction, Fig.10. This is a natural assumption as the stiffener profile is only subjected to a direct force in the longitudinal x-direction and is free to expand and contract in the z-direction. Though, second order membrane stresses may develop in all directions due to local buckling displacements out of the (x, z) plane. However, since the stiffener web plate is only supported by a stiffener flange (for T, L and bulb profiles) on the free edge, and a thin continuous plating on the other side, it is reasonable to eliminate all second order membrane stresses, except in the x-direction. This assumption is called a lower bound approach for plate buckling strength assessment and has been used by several authors, see e.g. Rhodes (1982).

The continuous plating in the (x,y) plane can be treated in more general terms with respect to the in-plane boundary conditions. For example if the panel is an integrated element in a deck field in a ship structure, it may be most realistic to prescribe straight edges free to move in-plane in the transverse direction. Such boundary conditions allow for full utilisation of second order tension and compression fields, which must be carried by neighbouring platefields. This type of boundary conditions is much used in the literature and is adopted for instance in Steen (1989). However, in the present model a simpler set of unconstrained in-plane boundary conditions is used. By using this more conservative edge condition for the longitudinal plate edges, lower elastic postbuckling stiffness in the local modes is available, see Rhodes (1982). However, since the purpose of the present model is to study the interactive buckling between overall and local buckling modes, such differences in in-plane boundary conditions is not an issue here. Thus, both the stiffener web plate and the continuous plating have been considered as plate elements with no ability to transmit second order transverse or shear membrane stresses. This simplifies the construction of the potential energy function, which have been used as the basis for the derivation of the local equilibrium equations.

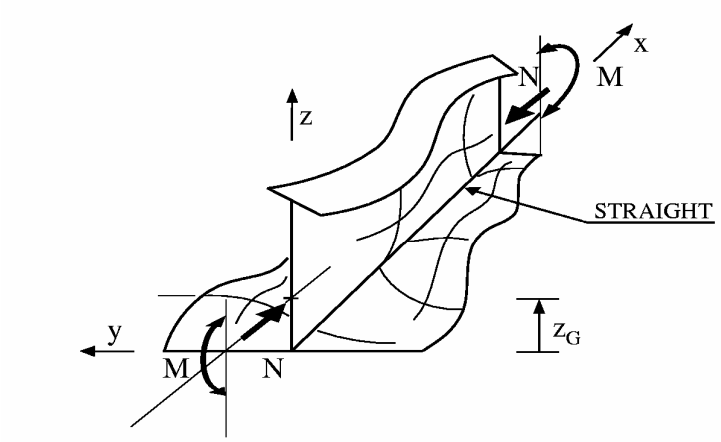

Fig.10. Local buckling modes and load system acting on a stiffened panel unit, schematically.

In Section 4.3.2 two local buckling modes typical for open profiles are described. Section 4.3.3 apply these modes as input to the Marguerre's compatibility equations, which solved gives the second order membrane stress distributions for the continuous plating and stiffener web plate. These membrane stress distributions are then used in Section 4.3.4 for deriving the final form of the *macro material model*. Section 4.3.5 presents a potential energy formulation giving the non-linear equilibrium equations for the cross-sectional response. Finally, Section 4.3.6 derives some closed form equilibrium solutions valid for geometrical perfect cross-sections.

4.3.2 Buckling modes

Two different local buckling modes for the column cross-section have been considered. They are given the notation q_1 and q_2 respectively and they have the following characteristics

1) q_1-mode: Sideways/torsional buckling of stiffener with associated local buckling of plate. Fig.11a.

2) q_2-mode: Local buckling of stiffener web with associated local buckling of plate. Fig.11b

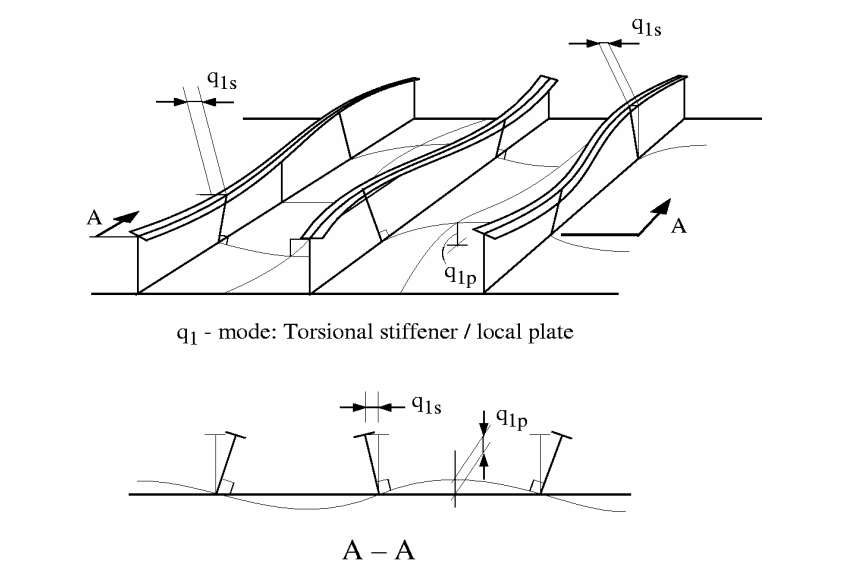

Fig.11a. Torsional stiffener/plate buckling mode

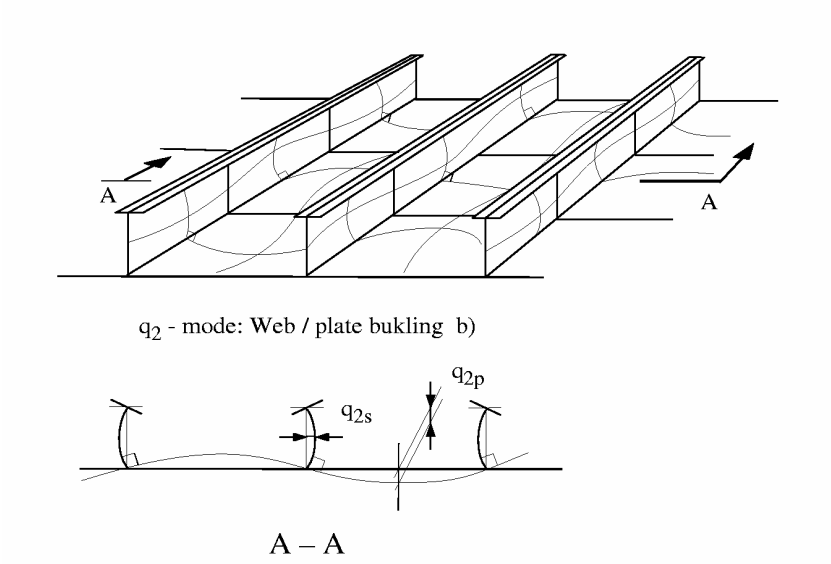

Fig. 11b. Stiffener web/plate buckling mode

The stiffener lateral deflection function w_s (perpendicular to x-z-plane) is assumed to take the form

$$w_s = t_w (q_{1s} \frac{z}{H} \sin \frac{\pi q}{L} x + q_{2s} \sin \frac{\pi p}{L} x \sin \frac{\pi}{H} z) \tag{64}$$

The plate lateral deflection function w_p is assumed to take the form

$$w_p = t_p (q_{1p} \sin \frac{\pi q}{L} x \sin \frac{\pi}{s} y + q_{2p} \sin \frac{\pi p}{L} x \sin \frac{\pi}{s} y) \tag{65}$$

The initial imperfection shapes are assumed to be in the same form as the buckling modes i.e. they are defined as

Stiffener:

$$w_{s0} = t_w (q_{10s} \frac{z}{H} \sin\frac{\pi q}{L} x + q_{20s} \sin\frac{\pi p}{L} x \sin\frac{\pi}{H} z) \tag{66}$$

Plate:

$$w_{p0} = t_p (q_{10p} \sin\frac{\pi q}{L} x \sin\frac{\pi}{s} y + q_{20p} \sin\frac{\pi p}{L} x \sin\frac{\pi}{s} y) \tag{67}$$

The deflection amplitudes q_{is}, q_{i0s} are made dimensionless with respect to the stiffener web thickness t_w. The deflection amplitudes q_{ip}, q_{i0p} are made dimensionless with respect to the plate thickness t_p. The height H represents the mean stiffener height and L is the stiffener span, see notation list.

The assumed buckling modes in Eq. (64) to Eq. (67) imply that the stiffener torsional and web buckling modes are associated with different wave numbers, p and q in the longitudinal direction. It follows that the plate displacement patterns are, per definition, constrained to follow the stiffener displacement patterns. The wave numbers p and q are found by minimising eigenvalues of the geometrically perfect cross-section (Appendix A5). They are kept fixed in the non-linear analysis, implying that local mode snapping is not dealt with. Also, as mentioned previously, the geometrical imperfection pattern is assumed to coincide with the minimum eigenmodes. This follows from the assumed shapes, Eq.(73) and Eq.(74).

The constraint of having the same wave numbers in stiffener and plate, together with the assumption of no relative rotation between these elements along their junction lines, gives a reduction of the local degrees of freedom from four to two. Mathematically the constraint condition of no relative rotation takes the form

$$w_{s,z}\Big|_{z=0} \equiv w_{p,y}\Big|_{y=0} \tag{68}$$

and the relations between the q_{is} and q_{ip} coefficients are derived as

$$\begin{aligned} q_{1p} &= \frac{t_w}{t_p}\frac{s}{H}\frac{1}{\pi} q_{1s} \\ q_{2p} &= \frac{t_w}{t_p}\frac{s}{H} q_{2s} \end{aligned} \tag{69}$$

In the subsequent equations the two independent displacement parameters q_1 and q_2 have been given the following meaning

$$\begin{aligned} q_1 &\equiv q_{1s} \qquad q_{10} \equiv q_{10s} \\ q_2 &\equiv q_{2s} \qquad q_{20} \equiv q_{20s} \end{aligned} \tag{70}$$

Substituting these definitions and constraints into Eq. (64) and Eq.(65) gives the final expressions for the local buckling modes as

Stiffener:

$$w_s = t_w (q_1 \frac{z}{H} \sin\frac{\pi q}{L} x + q_2 \sin\frac{\pi p}{L} x \sin\frac{\pi}{H} z) \tag{71}$$

Plate:

$$w_p = t_p (\frac{t_w}{t_p}\frac{s}{H}\frac{1}{\pi} q_1 \sin\frac{\pi q}{L} x \sin\frac{\pi}{s} y + \frac{t_w}{t_p}\frac{s}{H} q_2 \sin\frac{\pi p}{L} x \sin\frac{\pi}{s} y) \tag{72}$$

For the initial stress free initial imperfections the corresponding assumptions leads to

Stiffener:

$$w_{s0} = t_w (q_{10} \frac{z}{H} \sin\frac{\pi q}{L} x + q_{20} \sin\frac{\pi p}{L} x \sin\frac{\pi}{H} z) \tag{73}$$

Plate:

$$w_{p0} = t_p (\frac{t_w}{t_p}\frac{s}{H}\frac{1}{\pi} q_{10} \sin\frac{\pi q}{L} x \sin\frac{\pi}{s} y + \frac{t_w}{t_p}\frac{s}{H} q_{20} \sin\frac{\pi p}{L} x \sin\frac{\pi}{s} y) \tag{74}$$

The present assumptions for the local buckling modes are very simplified, but for a large range of parameter values, typical for stiffened plates used in ships and offshore structures, they will give reasonable strength estimates. They also have the benefit of providing some closed form postbuckling solutions as discussed in Chapter 5.

4.3.3 Membrane compatibility conditions

As mentioned previously, the solution of Marguerre's compatibility equation will give explicit expressions for the membrane stresses in a component plate. According to standard non-linear buckling theory, the membrane stresses in a plate have two contributions. The first contribution is the direct applied stresses while the second contribution is a periodic stress field due to plate buckling. Naturally the second order stresses integrated over the plate gives no contribution to the applied load, but they will add to the direct stresses giving higher stresses in certain locations, i.e. typically along the supported edges, intersections betweeen component plates etc. Locations with accumulated stresses are called hard corners positions. This latter concept is not pursued further in this report since it is most interesting in connection with inelastic material response (ref. Section 2.1).

In the present model the expressions for the membrane stresses in the continuous plating and in the stiffener web plate, respectively are found as two independent solutions of Marguerre's compatibility equation. The two separate compatibility equations are given as

Plating:

$$\nabla^4 F = E\left[(w_p + w_{p0})_{,xy}^2 - (w_p + w_{p0})_{,xx}(w_p + w_{p0})_{,yy} - (w_{p0,xy}^2 - w_{p0,xx}w_{p0,yy})\right] \qquad (75)$$

Stiffener web plate:

$$\nabla^4 F = E\left[(w_s + w_{s0})_{,xz}^2 - (w_s + w_{s0})_{,xx}(w_s + w_{s0})_{,zz} - (w_{s0,xz}^2 - w_{s0,xx}w_{s0,zz})\right] \qquad (76)$$

To find solutions to these compatibility equations is rather straight forward, but involves some tedious algebra, of which are not given here. The procedure is to substitute the derivatives of the displacement functions in Eq.(71) to Eq.(74) into the corresponding Eq. (75) and Eq.(76). Solving for Airy's stress function F and then using the definitions for the membrane stresses, Eq.(63), gives the analytical membrane stress expressions.

The consequence of formulating the membrane compatibility for the plating and stiffener web plate as two independent problems is that an assumption of a frictionless membrane connection is implicitly used. Said differently, the second order membrane stress and strain field in the plating and stiffener web plate is assumed to live their own lives with no transmit of second order shear stresses along the junction line (weld). This lack of full membrane strain compatibility along the junction line simplifies the model considerably and will give relaxed and conservative lower bound strength and stiffness values.

For the continuous plating the membrane stress distribution is found to be

$$\begin{aligned}\bar{\sigma}_x &= E[\varepsilon - z_G\kappa] \\ &- \left(\frac{E}{8}t_p^2\left[(R_1)^2\left(\frac{\pi q}{L}\right)^2(q_1^2 + 2q_1q_{10}) + (R_2)^2\left(\frac{\pi p}{L}\right)^2(q_2^2 + 2q_2q_{20})\right](1 - \cos\frac{2\pi}{s}y)\right. \\ &- Et_p^2(q_1q_2 + q_1q_{20} + q_2q_{10})\frac{((q+p)\pi/L)^2(\pi/s)^4}{(((q-p)\pi/L)^2 + (2\pi/s)^2)^2}\cos\frac{(q-p)\pi}{L}x\cos\frac{2\pi}{s}y \\ &+ \left.Et_p^2(q_1q_2 + q_1q_{20} + q_2q_{10})\frac{((q-p)\pi/L)^2(\pi/s)^4}{(((q+p)\pi/L)^2 + (2\pi/s)^2)^2}\cos\frac{(q+p)\pi}{L}x\cos\frac{2\pi}{s}y\right)\end{aligned} \qquad (77)$$

For the stiffener web plate the membrane stress distribution is found to be

$$\begin{aligned}\bar{\sigma}_x &= E[\varepsilon + (z - z_G)\kappa] \\ &- (\frac{E}{4}\left(\frac{\pi q}{L}\right)^2 t_w^2 (q_1^2 + 2q_1 q_{10})\left(\frac{z}{H}\right)^2 \\ &+ \frac{E}{4}\left(\frac{\pi p}{L}\right)^2 t_w^2 (q_2^2 + 2q_2 q_{20})(1 - \cos\frac{2\pi}{H} z))\end{aligned} \tag{78}$$

As discussed previously the transverse and shear membrane stresses are neglected in the analysis.

In compact form these membrane stress distributions can be given the notation of Eq.(44), i.e. they can be written as general stress functions

$$\bar{\sigma}_x = \bar{\sigma}_x^{\,plating}(\varepsilon, \kappa, q_i) \qquad \text{continuous plating, i = 1,2} \tag{79}$$

$$\bar{\sigma}_x = \bar{\sigma}_x^{\,web}(\varepsilon, \kappa, q_i) \qquad \text{stiffener web plate, i =1,2} \tag{80}$$

Within the present approximations, it is seen from Eq.(78) that the membrane stress in the stiffener web plate is quadratic in q_1 and q_2. Moreover, it has no x dependence. It is also observed that there is no coupling term $q_1 q_2$.

For the plate, Eq.(77), the situation is more complex in that the membrane stress pattern contains a coupling term $q_1 q_2$, which has a periodic x dependence. When the stress is integrated over the plate to find the total load, the coupling term vanishes and gives no contribution to the total load.

4.3.4 Macro material formulation for open sections

When the expressions for membrane stress pattern in each component plate is found, as in Section 4.3.3, it is straight forward to find the resulting axial force N and bending moment M. Substituting the membrane stress pattern, Eq.(77) and Eq.(78) into the definitions for the cross-sectional forces of N and M , Eq.(3), and carry out the integrations, the following functions emerge

$$\begin{aligned}N &= K_{11}^{\,L}\varepsilon + B_{11}(q_1^2 + 2q_{10}q_1) + B_{12}(q_2^2 + 2q_{20}q_2) \\ M &= K_{22}^{\,L}\kappa + B_{21}(q_1^2 + 2q_{10}q_1) + B_{22}(q_2^2 + 2q_{20}q_2)\end{aligned} \tag{81}$$

Eq.(81) is the final form of the present two-dimensional *macro material model* (N, M) described by two-degrees of freedom q_1 and q_2 for the local cross-sectional buckling modes. In matrix notation Eq.(81) can be written as

$$\begin{bmatrix} N \\ M \end{bmatrix} = \begin{bmatrix} K_{11}^{\,L} & 0 \\ 0 & K_{22}^{\,L} \end{bmatrix} \begin{bmatrix} \varepsilon \\ \kappa \end{bmatrix} + \begin{bmatrix} B_{11} & B_{12} \\ B_{21} & B_{22} \end{bmatrix} \begin{bmatrix} q_1^{\,2} + 2q_1 q_{10} \\ q_2^{\,2} + 2q_2 q_0 \end{bmatrix} \tag{82}$$

The K_{11}^{L} and K_{22}^{L} are the linear stiffness coefficients defined in Eq.(12a). The B_{11}, B_{12}, B_{21} and B_{22} are geometrical coefficients given in Appendix 6.

By using the definitions for the current stiffness coefficients, Eq.(50), and Eq.(81), the final expressions for the first order stiffness coefficients are found as

$$\begin{aligned}
K_{11} &= K_{11}^{L} + 2B_{11}(q_1 + q_{10})\frac{\partial q_1}{\partial \varepsilon} + 2B_{12}(q_2 + q_{20})\frac{\partial q_2}{\partial \varepsilon} \\
K_{12} &= K_{12}^{L} + 2B_{11}(q_1 + q_{10})\frac{\partial q_1}{\partial \kappa} + 2B_{12}(q_2 + q_{20})\frac{\partial q_2}{\partial \kappa} \\
K_{21} &= K_{21}^{L} + 2B_{21}(q_1 + q_{10})\frac{\partial q_1}{\partial \varepsilon} + 2B_{22}(q_2 + q_{20})\frac{\partial q_2}{\partial \varepsilon} \\
K_{22} &= K_{11}^{L} + 2B_{21}(q_1 + q_{10})\frac{\partial q_1}{\partial \kappa} + 2B_{22}(q_2 + q_{20})\frac{\partial q_2}{\partial \kappa}
\end{aligned} \tag{83}$$

In a numerical perturbation procedure, evaluation of the current K_{ij} coefficients will follow the scheme as presented in Section. 3.1.

In Chapter 5 closed form solutions, based on Eq.(83) for the case of geometrical perfect cross-sections are derived for some specific examples and comparisons are made with solutions found in the literature.

The next section describes the derivations of the equilibrium equations for the local cross-sectional buckling problem in the q_1 and q_2 mode.

4.3.5 Equilibrium formulation

The purpose of this section is to formulate a set of local equilibrium equations in the form as given by Eq.(53). There are several ways to derive such equations, but the principle of stationary potential energy is a convenient method and applied here. The potential energy approach makes the formulation compact and it naturally fits into the form of non-linear finite-degree-of-freedom discrete stability theory developed by Croll and Walker (1972), Thompsen and Hunt (1973), Huseyin (1975) and others.

The potential energy of the stiffened plate is calculated for the unit as shown in Fig.8. Assumptions for the buckling modes, compatibility conditions and internal membrane stress distributions are as formulated in Section 4.3.2 and Section 4.3.3 respectively. Moreover, as was discussed in Section 3.1 the macro formulation is most conveniently formulated as a *displacement control* case. The potential energy of the cross-sectional unit under prescribed edge-deflections ε and κ is

$$V_{unit} = \frac{1}{2}\iiint \bar{\sigma}_{ij}\bar{\varepsilon}_{ij}\, dx\, dy\, dz \tag{84}$$

Since the analysis is done with displacement control (ε, κ), no external load potential exist. Note that in Eq.(84) tensor notation for symbolising the stress and strains $\bar{\sigma}_{ij}, \bar{\varepsilon}_{ij}$ locally in a material point has been used.

The integration of the strain energy over the plate and stiffener unit has separate terms; i.e. the strain energy for the continuous plating, the stiffener web plate and stiffener flange are separate integrals.

As discussed in Section 4.3.1, the plate and stiffener elements are considered to behave in a pure uni-axial manner also when buckling is considered. Koiter (1971) first used this approach, and it has been classified as a lower bound method for the postbuckling assessment as discussed by Rhodes (1982). Using the thin shell theory described in Section 4.2, and a pure uni-axial material law ($\bar{\sigma}_{11} = E\bar{\varepsilon}_{11}$) in both plate and stiffener, gives the following expression for the potential energy under prescribed axial deflection

$$
\begin{aligned}
V_{unit} = {} & \frac{E\, t_p^{\,3}}{24(1-\nu^2)} \iint_{Plate} \left[w_{,xx}^2 + w_{,yy}^2 + 2\nu w_{,xx} w_{,yy} + 2(1-\nu) w_{,xy}^2 \right] dx\, dy \\
& + \frac{t_p}{2E} \iint_{Plate} \bar{\sigma}_x^2 \, dx\, dy \\
& + \frac{E t_w^3}{24(1-\nu^2)} \iint_{Stiff.web} \left[w_{,xx}^2 + w_{,zz}^2 + 2\nu w_{,xx} w_{,zz} + 2(1-\nu) w_{,xz}^2 \right] dx\, dz \\
& + \frac{t_w}{2E} \iint_{Stiff.web} \bar{\sigma}_x^2 \, dx\, dz \\
& + \frac{EI_f}{2} \int_{Stiff.flange} w_{,xx|\, z=H}^2 dx \\
& + \frac{GJ_p}{2} \int_{Stiff.flange} w_{,xz|z=H}^2 dx \\
& + \frac{A_f}{2E} \int_{Stiff.flange} \bar{\sigma}_{x|\, z=H}^2 dx
\end{aligned}
\qquad (85)
$$

I_f and J_p are the moment of inertia and torsional constant of the stiffener flange, respectively. The parameter A_f is the cross sectional area of the stiffener flange, t_p is the plate thickness and t_w is stiffener web plate thickness. For a complete definition of parameters see the notation list.

When applying the thin-shell theory approximations and choosing the middle-planes to be the reference planes, the strain energy expression, Eq.(85), is split into a separate bending and membrane contribution for each component plate. The bending contribution is a second order function in the curvature of the element reference surface meaning that it is a quadratic function of the local displacement parameters q_i. The membrane contribution is a second

order function of the membrane stress $\overline{\sigma}_x$ in the plate middle-plane meaning a quartic function in the displacement parameters q_i. This is well known properties in buckling theory of plates, see e.g. Brush and Almroth (1975).

Substituting the assumed deflection functions, expressions for the membrane stresses and constraint condition between plate and stiffener, given in Section 4.3.2 and 4.3.3 respectively into Eq.(85), the final expression for the potential energy is found to be

$$
\begin{aligned}
&V(\varepsilon,\kappa,q_1,q_2) = \\
&\\
&+a_4(q_1)^4 \\
&+a_3 q_{10}(q_1)^3 \\
&+a_{21}(q_1)^2 + a_{22}(q_{10})^2(q_1)^2 \\
&\\
&+b_4(q_2)^4 \\
&+b_3 q_{20}(q_2)^3 \\
&+b_{21}(q_2)^2 + b_{22}(q_{20})^2(q_2)^2 \\
&\\
&+c_4(q_1)^2(q_2)^2 \\
&+c_{31}q_{10}q_1(q_2)^2 + c_{32}q_{20}q_2(q_1)^2 \\
&+c_{21}q_{10}q_{20}q_1q_2 + c_{22}(q_{20})^2(q_1)^2 + c_{23}(q_{10})^2(q_2)^2 \\
&\\
&+g_{1u}(q_1)^2\varepsilon + g_{1u0}q_{10}q_1\varepsilon + g_{1\theta}(q_1)^2\kappa + g_{1\theta0}q_{10}q_1\kappa \\
&+g_{2u}(q_2)^2\varepsilon + g_{2u0}q_{20}q_2\varepsilon + g_{2\theta}(q_2)^2\kappa + g_{2\theta0}q_{20}q_2\kappa \qquad (86) \\
&\\
&+h_{uu}\varepsilon^2 + h_{u\theta}\varepsilon\kappa + h_{\theta\theta}\kappa^2
\end{aligned}
$$

The a, b, c and g and h coefficients (with subscripts) are all rather complicated geometrical constants and they are given in Appendix A1.

The potential energy function V is a quartic function in the q_1 and q_2 modes with a quartic coupling term $q_1^2q_2^2$. Moreover V has terms $q_1^2\varepsilon$, $q_1^2\kappa$, $q_2^2\varepsilon$, $q_2^2\kappa$ all linear in the control displacement parameters ε and κ. V has also a set of constant terms, i.e. the second order terms in ε and κ. These latter terms have no importance and vanish when the equilibrium equations are derived.

Applying the principle of stationary potential energy, i.e.

$$\begin{aligned}\frac{\partial V}{\partial q_1} &= 0\\ \frac{\partial V}{\partial q_2} &= 0\end{aligned} \tag{87}$$

gives the following two equilibrium equations

$$\begin{aligned}V_1 = &\\ &+ 4a_4(q_1)^3\\ &+ 3a_3 q_{10}(q_1)^2\\ &+ 2a_{21}q_1 + 2a_{22}(q_{10})^2 q_1\\ &\\ &+ 2c_4 q_1(q_2)^2\\ &+ c_{31}q_{10}(q_2)^2 + 2c_{32}q_{20}q_2 q_1\\ &+ c_{21}q_{10}q_{20}q_2 + 2c_{22}(q_{20})^2 q_1\\ &\\ &+ 2g_{1u}q_1\varepsilon + g_{1u0}q_{10}\varepsilon + 2g_{1\theta}q_1\kappa + g_{1\theta 0}q_{10}\kappa = 0\end{aligned} \tag{88}$$

$$\begin{aligned}V_2 = &\\ &+ 4b_4(q_2)^3\\ &+ 3b_3 q_{20}(q_2)^2\\ &+ 2b_{21}q_2 + 2b_{22}(q_{20})^2 q_2\\ &\\ &+ 2c_4 q_2(q_1)^2\\ &+ 2c_{31}q_{10}q_1 q_2 + c_{32}q_{20}(q_1)^2\\ &+ c_{21}q_{10}q_{20}q_1 + 2c_{23}(q_{10})^2 q_2\\ &\\ &+ 2g_{2u}q_2\varepsilon + g_{2u0}q_{20}\varepsilon + 2g_{2\theta}q_2\kappa + g_{2\theta 0}q_{20}\kappa = 0\end{aligned} \tag{89}$$

V_1 and V_2 symbolised the partial derivatives of V with respect to q_1 and q_2 respectively.

Eq.(88) and Eq.(89) constitute two non-linear cubic equilibrium equations in the two unknowns q_1 and q_2. In the present formulation they are the equations generally written in the form of Eq.(53).

4.3.6 Equilibrium solutions

When discussing and presenting equilibrium solutions it is important to define under which conditions they apply. As the title of the present chapter reveals, only local cross-sectional buckling is considered and this applies also for the solutions given in the following. Chapter 5 presents some specific solutions, which also consider the coupling with the overall column mode.

The displacement control option is selected in this study since this gives directly the stiffness parameters as defined in Eq.(50). The difference between load control and displacement control is more discussed in Steen(1998).

There exist no analytical closed form solution for the set of cubic equilibrium equations, Eq.(88), Eq.(89). However, setting the initial imperfection amplitudes to zero ($q_{10} = q_{20} = 0$), we obtain the two equilibrium equations as

$$\begin{aligned} q_1(4a_4(q_1)^2 + 2a_{21} + 2c_4(q_2)^2 + 2g_{1u}\varepsilon + 2g_{1\theta}\kappa) = 0 \\ q_2(4b_4(q_2)^2 + 2b_{21} + 2c_4(q_1)^2 + 2g_{2u}\varepsilon + 2g_{2\theta}\kappa) = 0 \end{aligned} \tag{90}$$

This set of equations has 4 separate solutions as follows

Solution 1: no buckling

$$q_1 = q_2 = 0 \qquad \text{i.e. - prebuckling solution} \tag{91}$$

Solution 2: - Single mode buckling in q_2

$$q_1 = 0, \qquad q_2^{\,2} = -\frac{1}{2b_4}(b_{21} + g_{2u}\varepsilon + g_{2\theta}\kappa) \tag{92}$$

Solution 3: - Single mode buckling in q_1

$$q_2 = 0, \qquad q_1^{\,2} = -\frac{1}{2a_4}(a_{21} + g_{1u}\varepsilon + g_{1\theta}\kappa) \tag{93}$$

Solution 4: - Coupled mode in q_1 and q_2

$$\begin{aligned} (q_1)^2 &= \frac{1}{4a_4 - (c_4)^2/b_4}\left[-(2a_{21} - \frac{c_4}{b_4}b_{21}) + (\frac{c_4}{b_4}g_{2u} - 2g_{1u})\varepsilon + (\frac{c_4}{b_4}g_{2\theta} - 2g_{1\theta})\kappa\right] \\ (q_2)^2 &= \frac{1}{4b_4 - (c_4)^2/a_4}\left[-(2b_{21} - \frac{c_4}{b_4}a_{21}) + (\frac{c_4}{a_4}g_{1u} - 2g_{2u})\varepsilon + (\frac{c_4}{a_4}g_{1\theta} - 2g_{2\theta})\kappa\right] \end{aligned} \tag{94}$$

Solution 1 corresponds to no buckling and needs no specific comments. Solution 2, 3 and 4 are closed form solutions for the buckling mode amplitudes for given prescribed deflection parameters ε and κ. They can be visualised as equilibrium surfaces schematically illustrated in Fig.12. These equilibrium surfaces have the classical parabolic shape as known from the Koiter theory.

The most significant result is solution 4, which gives an explicit closed form solution for the case of a coupled simultaneous cross-sectional buckling response into mode q_1 and mode q_2. The solution gives two parabolic equilibrium surfaces which intersect in the four dimensional solution space (q_1, q_2, ε, κ).

The present study does not present any mathematical study of these surfaces and possible equilibrium paths across them, as this beyond the scope of the present work. However, based on the same closed form solution, Bangstein (1996) discussed some practical consequences. He found that for a hinged stiffener (setting the plate area to zero), the non-linear interaction between torsional stiffener and web buckling gave in-plane axial postbuckling stiffness properties well below the corresponding stiffness values found in the separate modes.

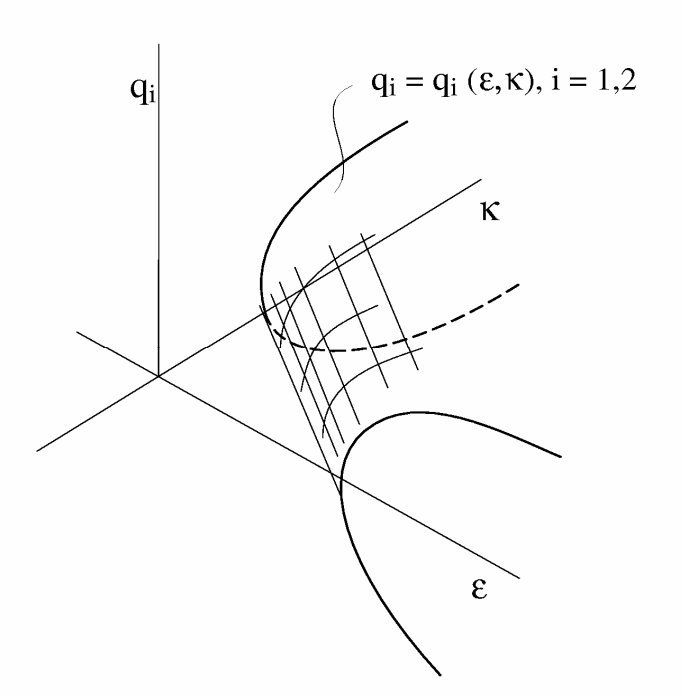

Fig.12 Single mode equilibrium surface schematically illustrated – perfect geometry

As already emphasised, the closed form solutions, Eq.(92), Eq.(93), Eq.(94) assumes the cross-section to be geometrically perfect. This leads to very simple and useful closed form expressions for a qualitative study of postbuckling stiffness. This is explored in the next section.

4.3.7 Stiffness properties

In Section 2.2 the stiffness properties of locally buckled cross-sections were introduced as the tangent stiffness coefficients K_{ij} and Section 2.4 and 2.5 showed the importance of these coefficients in determining the coupled local and overall buckling response of columns. This section gives a mathematical representation of these stiffness coefficients, as an alternative and possibly useful point of view for illuminating their importance.

By using the closed form solutions derived above for geometrical perfect cross-sections it is straightforward to show that the K_{ij} coefficients emerge as constants. Substituting Eq.(92) (or Eq.(93), Eq.(94)) into Eq.(81) and using the definition of Eq.(9) it follows directly that the incremental loads ΔN and ΔM and the corresponding displacements $\Delta\varepsilon$ and $\Delta\kappa$ is related by a *linear macro material law*. This incremental macro law can be written in matrix notation as

$$\begin{bmatrix} \Delta N \\ \Delta M \end{bmatrix} = \begin{bmatrix} K_{11} & K_{12} \\ K_{21} & K_{22} \end{bmatrix} \begin{bmatrix} \Delta\varepsilon \\ \Delta\kappa \end{bmatrix} \tag{95}$$

As in Section 2.5 the Δ symbol indicates incremental properties along the postbuckling equilibrium surfaces and the K_{ij} are constant coefficients. The complete expressions of these coefficients are given Appendix A7.

As explained in Section 3.1, the form of Eq.(95) includes the equilibrium solution, and the displacement vector q_i is not visible. In a mathematical language, the functions of Eq.(95), can be viewed as two-dimensional surfaces in the three dimensional spaces (N, ε, κ) and (M, ε, κ) respectively. In the most general non-linear version the stiffness solutions have the form of Eq.(6), here repeated as

$$\begin{aligned} N &= N(\varepsilon, \kappa) \\ M &= M(\varepsilon, \kappa) \end{aligned} \tag{96}$$

By mapping these functions into the deflection space (ε,κ) as contour plots, the stiffness of the cross-sectional response appears as the gradient to fixed contour lines, see Steen (1998).

As indicated for the present local cross-sectional buckling study, the significant finding is that the K_{ij} coefficients are constants and not load-dependent in the postbuckling region. Mathematically this means that the contour plots will be straight lines in the displacement space (ε, κ).

Contour plots are schematically illustrated in Fig.13. In Fig.13a the gradient to the contour lines of fixed load N values, in the (ε, κ) space, are given by the mathematical equation

$$\text{grad}\Delta N = K_{11}\mathbf{i}_\varepsilon + K_{12}\mathbf{i}_\kappa \tag{97}$$

Here the stiffness coefficients K_{11} and K_{12} are the components of the gradient to the function N in the unit displacement directions ε and κ, respectively. In Fig.13 the unit vectors $\mathbf{i}_\varepsilon$ and $\mathbf{i}_\kappa$ are oriented along the ε-axis and κ-axis respectively.

A similar stiffness gradient for the moment function M can be constructed and schematically illustrated in Fig.13b. In mathematical terms the M gradient can be written as

$$\text{grad}\Delta M = K_{21}\mathbf{i}_{\varepsilon} + K_{22}\mathbf{i}_{\kappa} \tag{98}$$

In Eq.(98) the stiffness coefficients K_{21} and K_{22} are the components of the moment gradient in the unit directions ε and κ respectively.

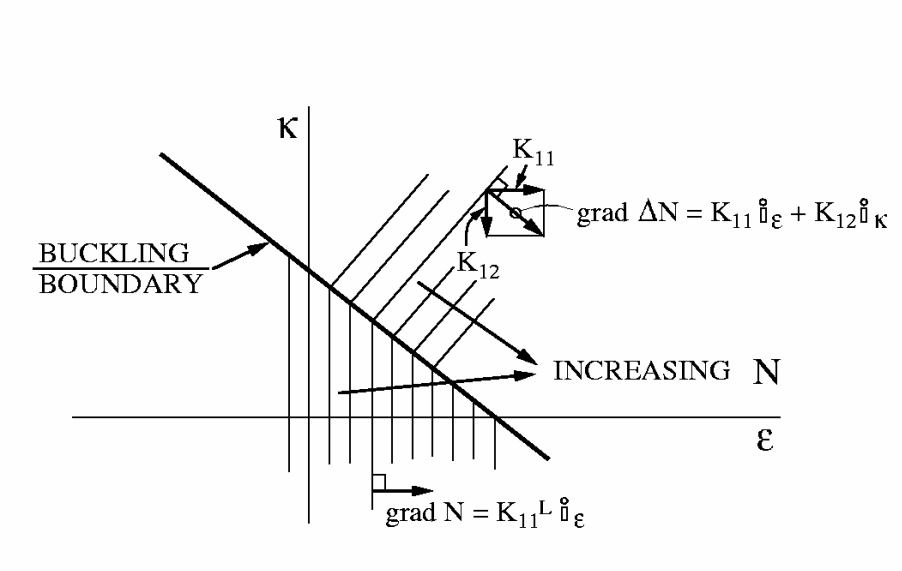

a) Contour plot for fixed N values

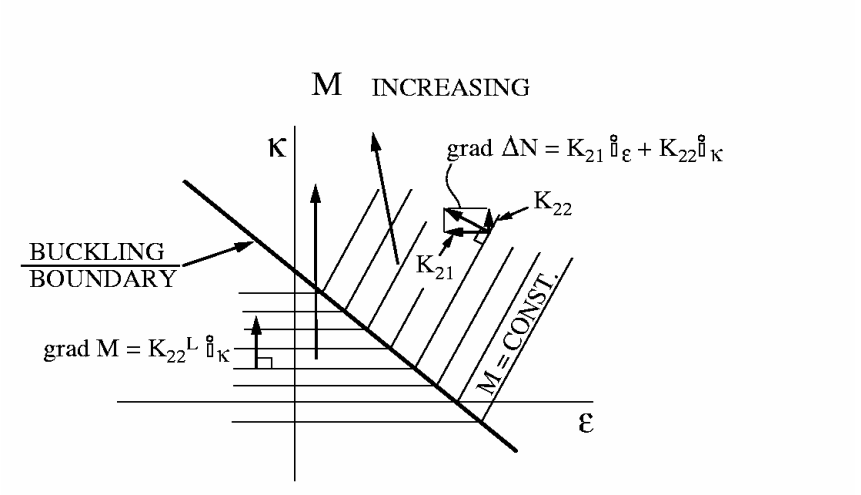

b) Contour plot for fixed M values

Fig. 13. Stiffness contour plots for load N and moment M.
a) Contour lines ; Force N = constants, b) Contour lines; Moment M = constants

It is emphasised that Fig.13 is only a schematic illustration of cross-sectional stiffness properties in terms of contour plots. The thick line is indicating the (eigenvalue) buckling boundary separating the prebuckling and postbuckling region. It is worth mentioning that this buckling boundary normally will be a convex curve seen from origo. Thin lines represent fixed N (or M) values.

For a cross-section with geometrical imperfections the equilibrium surfaces will be continuous. Under such conditions the contour lines will be mapped as continuous curves in space (ε, κ), smoothing out the region between prebuckling and postbuckling states.

From a physical point of view, it was illustrated in Chapter 2 that the values of the stiffness coefficients K_{ij} were very important for capturing the non-linear structural interaction between local and overall buckling. The present discussion has emphasised that the stiffness coefficients K_{ij} can be viewed as contour plots of mathematical functions. Whether this illustration is of any direct use is a matter of taste, but at least it gives an understanding of the importance of the shape of these surfaces. From a physical point of view it is obvious that the requirement to accuracy of these surfaces is not equally strict in all regions of the (ε, κ) space. Since overall buckling of the present column model starts from the ε-axis, it will be most important to have an optimal accuracy for the contour lines along this axis. This conclusion support the relevance of the equilibrium solutions for the K_{ij} coefficients presented in this chapter (and also some special solutions in Chapter 5), which is founded on some qualified approximations for the buckling mode shapes typical for panels subjected to dominating axial compression and marginal cross-sectional bending.

4.4 Summary and discussion

The chapter starts with a brief introduction to Marguerre's non-linear plate theory, which is used as basis for the derivation of the cross-sectional macro material model.

The rest of the chapter is specifically devoted to the derivation of a two-dimensional *macro material model* for the case of a thin walled cross-section with an open profile shape, typically found in panels in ship and offshore constructions. The macro material model is approximated as a two-degree of freedom model for a compact treatment of the buckling and postbuckling strength. Torsional and web stiffener buckling modes are considered, both interacting with a plate buckling mode.

A significant result was the derivation of the macro material coefficients for the case of a geometrically perfect cross-section. Under such conditions it was shown that the macro material coefficients in the postbuckling region K_{ij} were *constants*, i.e. they were shown to be load-independent in the postbuckling region. The result of constant macro material coefficients validate the concept of the reduced modulus load as a safe lower bound limit for columns and stiffened panels, eliminating unstable postbuckling behaviour.

The concept of tangent stiffness coefficients was discussed from a mathematical point of view using contour lines of equilibrium surfaces. This emphazied the importance of the shape of

the equilibrium surfaces in certain regions. Though not discussed in detail here, it is obvious that the density and orientation of the equilibrium contour lines in this stiffness spaces will be vital for the degree of instability to be expected for the coupled local and overall buckling reponse.

Naturally, the present finding of fixed and load-independent stiffness coefficients for perfect cross-sections, rest on some very simplified assumptions. Nevertheless, it may be postulated that the main physical behaviour is captured and that the present derived properties will be very typical for thin-walled built up sections. Thus the present macro model may prove to be useful for semi-theoretical design approaches. As verification of the present results, some comparisons with results found in the literature are given in Chapter 5.

5. DISCUSSION - VERIFICATION

5.1 General

The main purpose of the present work was to develop a simplified numerical buckling model that could handle the severe unstable interaction between local cross-sectional and overall buckling in stiffened panels. The presents proposed solution to this problem consist of applying a macro material model concept for the pure local geometrical response and using a general section Shanley model for coupling the overall response to the local. Thus it is convenient to see the model having two separate parts

i) Macro material model for local buckling and postbuckling response assessment.
ii) Buckling model (here Shanley) for coupling of local and overall buckling.

In order to verify the model results, comparisons have been carried out at these two levels.

There exist few studies in the literature, which can be categorised as pure macro material models formulations and therefore very few comparable solutions are available. However, some closed form solutions exist notably derived by Stowell (1951) and Rhodes (1982). In addition Ellinas and Croll (1981) presented some numerical solutions for the reduced modulus factor for torsional buckling of stiffeners.

For the coupled local and overall buckling case, a closed form solution by Rhodes (1982) can be used for direct comparison purposes. This is the only directly comparable closed-formed solution found in the literature and it represents an extreme and not very practical case. In order to illustrate more practical cases the present numerical model has been tested on two examples. The basis is the macro model developed in Chapter 4 combined with the numerical incremental perturbation scheme presented in Section 3.2. The first example has typical dimensions as used in decks in large steel ships while the second example is constructed in order to illustrate the unstable response when buckling into a simultaneous local and overall column buckling mode takes place.

5.2 Macro material solutions

5.2.1 Single mode solution

By using Eq.(88), and setting $q_2 = q_{20} = 0$ the following single mode solution (see Appendix A3), can be derived

$$L_\varepsilon \varepsilon + L_\kappa \kappa = \frac{q_1}{q_1 + q_{10}}(1 + b_2(q_1^{\,2} + 3q_1 q_{10} + 2q_{10}^{\,2})) \tag{99}$$

In Eq.(99) the parameters L_ε, L_κ are geometrical constants and b_2 is Koiter's postbuckling coefficient for symmetric structures. The single mode solution written in the form of Eq.(99) differs from the classical Koiter solution (see e.g. Dym (1974)) in the two imperfection terms $3q_1 q_{10} + 2q_{10}^{\,2}$ given within the parenthesis. Koiter's solution is only strictly valid for very small imperfection levels while the present solution has a wider range of validity.

The single mode version of Eq.(83) for the macro material coefficients K_{ij} is

$$\begin{aligned}
K_{11} &= K_{11}^{\,L} + 2B_{11}(q_1 + q_{10})\frac{\partial q_1}{\partial \varepsilon} \\
K_{12} &= K_{12}^{\,L} + 2B_{11}(q_1 + q_{10})\frac{\partial q_1}{\partial \varepsilon} \\
K_{21} &= K_{21}^{\,L} + 2B_{21}(q_1 + q_{10})\frac{\partial q_1}{\partial \kappa} \\
K_{22} &= K_{22}^{\,L} + 2B_{21}(q_1 + q_{10})\frac{\partial q_1}{\partial \kappa}
\end{aligned} \tag{100}$$

The partial derivatives $\partial q_1 / \partial \varepsilon$, $\partial q_1 / \partial \kappa$ is from Eq.(51)

$$\begin{aligned}
\frac{\partial q_1}{\partial \varepsilon} &= -\frac{\partial f_1 / \partial \varepsilon}{\partial f_1 / \partial q_1} \\
\frac{\partial q_1}{\partial \kappa} &= -\frac{\partial f_1 / \partial \kappa}{\partial f_1 / \partial q_1}
\end{aligned} \tag{101}$$

in which f_1 is defined as

$$f_1(\varepsilon, \kappa, q_1) = L_\varepsilon \varepsilon + L_\kappa \kappa - \frac{q_1}{q_1 + q_{10}}(1 + b_2(q_1^{\,2} + 3q_1 q_{10} + 2q_{10}^{\,2})) \tag{102}$$

Using Eq.(101) and Eq.(102) it can be shown that the first order stiffness coefficients K_{ij} can be written in the following compact closed form

$$
\begin{aligned}
K_{11} &= K_{11}^{\,L} + 2B_{11}(q_1 + q_{10})L_\varepsilon\Omega \\
K_{12} &= K_{12}^{\,L} + 2B_{11}(q_1 + q_{10})L_\kappa\Omega \\
K_{21} &= K_{21}^{\,L} + 2B_{21}(q_1 + q_{10})L_\varepsilon\Omega \\
K_{22} &= K_{22}^{\,L} + 2B_{21}(q_1 + q_{10})L_\kappa\Omega
\end{aligned}
\qquad (103)
$$

where

$$
\Omega = \frac{(q_1 + q_{10})^2}{q_{10} + 2b_2(q_1 + q_{10})^3} \qquad (104)
$$

The form of Eq.(103) is valid for any single degree of freedom system with the geometrical constants B_{11}, B_{21}, L_ε, L_κ, and b_2 as case dependent.

The present single mode solution gives explicit expressions for the macro material coefficients K_{ij}. This is a useful property for fast implementation in computerised design models.

5.2.2 Closed-form solution - Plate with one longitudinal edge free

In order to obtain simple closed-formed solutions it is of interest to study the case of a rectangular plate with one longitudinal edge free and the other three simply supported. This plate problem can be interpreted as identical to a flat bar profile attached to plating with no axial stiffness. This plate problem was first studied by Stowell(1951) and later by Rhodes (1982) who included also the overall buckling effect. Comparisons with these publications are therefore included. For the full solution of open profiles attached to a plating with axial stiffness, see Appendix A7.

For the isolated flat bar stiffener the geometrical constants B_{11}, B_{21}, L_ε, L_κ, ε_C and b_2 take the following values

$$
\begin{aligned}
B_{11} &= -\frac{\pi^2}{12}E\left(\frac{t_w}{L}\right)^2 H\, t_w \\
B_{21} &= -\frac{\pi^2}{48}E\left(\frac{t_w}{L}\right)^2 H^2\, t_w
\end{aligned}
\qquad (105)
$$

$$
\begin{aligned}
L_\varepsilon &= \frac{1}{\varepsilon_C} \\
L_\kappa &= \frac{1}{4}H\frac{1}{\varepsilon_C}
\end{aligned}
\qquad (106)
$$

$$\varepsilon_C = \frac{\pi^2}{12(1-\nu^2)}\left(\frac{t_w}{H}\right)^2\left[\frac{6(1-\nu)}{\pi^2}+\left(\frac{H}{L}\right)^2\right]$$
$$b_2 = \frac{3\pi^2}{20}\left(\frac{t_w}{L}\right)^2\frac{1}{\varepsilon_C} \qquad (107)$$

The linear stiffness coefficients follows from Eq.(12), i.e. with the present notation for stiffener web thickness t_w and height H, they become

$$K_{11}^{\ L} = E\,H\,t_w$$
$$K_{12}^{\ L} = 0$$
$$K_{21}^{\ L} = 0 \qquad (108)$$
$$K_{22}^{\ L} = \frac{1}{12}E\,H^3 t_w$$

Substituting the expressions for geometrical constraints, i.e. Eq.(105) to Eq.(108), into Eq.(103) and setting $q_{10} = 0$ the final expressions for the stiffness coefficients where found to be

$$K_{11} = \frac{4}{9}(EA_T)$$
$$K_{12} = K_{21} = -\frac{5}{18}\sqrt{3}\sqrt{(EA_T)(EI_T)} \qquad (109)$$
$$K_{22} = \frac{7}{12}(EI_T)$$

It follows directly from Eq.(109) that the postbuckling stiffness in pure axial compression, under axial displacement control (prescribed $\kappa = 0$), is

$$\frac{K_{11}}{K_{11}^{\ L}} = \frac{4}{9} \qquad (111)$$

This is the same value as originally given by Stowell(1951).

Despite the academic interest of the present simple plate buckling problem it is reassuring that the present solution converge towards recognised solutions found in the literature. Similar comparisons for the coupled local and overall buckling are given in Section 5.3.2.

5.2.3 Numerical results and comparisons with other solutions

Ellinas and Croll (1981) presented numerical results for the reduced modulus factor for stiffened plates buckling into a torsional/sideways stiffener mode. They developed a numerical scheme, solving the von Karman plate equations with due consideration of the boundary conditions between the stiffener web plate, top flange and bottom plate. The plating and stiffener bulb flange was treated as beams. They compared their theoretical results with small-scale model experiments made of Araldite, in order to capture the pure non-linear elastic response. They demonstrated very good correlation between theory and experiments and it was shown that the reduced modulus factor was of the order of 0.15-0.20 for the cases they studied.

Even though the geometrical proportions of the experimental models of Ellinas and Croll are small, and the relative slenderness ratio (h_w / t_w) of the stiffener web plate are very much higher than what is typical for ship and offshore structures, comparisons are interesting from a qualitative point of view. Therefore the present macro model developed in Chapter 4 was used to calculate the reduced modulus factors for the Ellinas and Croll examples and the comparisons are shown in Table 5.1.

Data	Case1 – Flat bar	Case 2 – Sym. Bulb
t_p [mm]	1.73	1.73
s [mm]	100	100
t_w [mm]	1.8	1.8
h_w [mm]	74	59
t_f [mm]	0	5.15
b_f [mm]	0	15.1
L [mm]	125	125
Reduced modules η_{BR}, Ellinas and Croll (1981)	**0.203**	**0.150**
Reduced modules η_{BR}, present macro model	**0.194**	**0.124**

Table 5.1 Comparisons between calculated reduced modulus factors η_{BR};, present macro model versus Ellinas and Croll (1981).

The comparisons in Table 5.1 shows very good correspondence and the severe bending stiffness reductions for very slender stiffeners (high h_w/t_w ratios, 41 and 33 respectively) buckling in a torsional/sideways buckling mode is documented. It is noted that the symmetric bulb profile has an even lower reduced modulus factor than the flat bar profile. This is natural since when first buckling of a bulb profile takes place, the bulb area itself loose relatively more of its axial efficiency compared to for instance cross-sectional area located closer to the edge support. A bulb profile will have a higher ideal elastic local buckling stress than a flat bar profile of the nominal same dimensions, but that is another discussion and not a part of the postbuckling characteristics evaluated here.

Moreover, Ellinas and Croll (1981) observed from their numerical model studies that the reduced modulus factor was *constant* for large deformations and thus independent of the value of the acting prescribed axial load level P. They concluded that the incremental moment-curvature relationship was a constant relationship in the postbuckling region. This is the same conclusion as found in the present study, here though founded solely on a closed form solution.

In short it can be concluded that the stiffness properties of locally buckled cross-sections are independent of the level of buckling displacements. This conclusion is based on limited studies and simplifying assumptions, but at least for cross-sections where a single mode analysis is sufficient, the constant postbuckling stiffness is a realistic feature. For cross-sections where several local buckling modes will interact, multi-linear postbuckling stiffness properties are likely. Eq.(94) indicates this, but this topic is not pursued further in this report.

5.3 Coupled local and overall buckling solutions

5.3.1 General

This section starts with a brief presentation of the closed form solutions for coupled local and overall buckling derived in Sections 2.4 and Section 2.5. Specialising these general section solutions for the particular simple case defined in Section 5.2.2 interesting features are revealed.

Then two numerical examples are presented, using the macro material model model developed in Chapter 4 in combination with the numerical scheme described in Section 3.2. Both local and overall geometrical imperfections are studied and the results are presented as load-shortening curves.

The two numerical examples have very different geometrical layout of plate and stiffener proportions and different types of structural response are illustrated. The first example is a typical geometrical layout used in decks in steel ships while the second example is a constructed case for illustrating the capability of the model to trace complex unstable postbuckling behaviour. By studying the load-shortening response of these examples, and by varying the magnitude of the geometrical imperfections, important observations can be extracted with respect to both structural strength and stiffness properties.

5.3.2 Closed form solution – Plate with one longitudinal edge free

In Section 5.2.2 a closed-formed solution for the postbuckling stiffness coefficients K_{ij} were given for a plate with one longitudinal edge free and other three simply supported. This example is continued in this section by presenting closed-formed solutions that includes the coupling effect with the overall buckling mode.

For overview of the presentation the general section solutions given in Section 2.4 are repeated here, i.e. Eq.(23), Eq.(24),(25) are rewritten in the forms as the load-curvature relation

$$\Delta P = S_\kappa \Delta\kappa \tag{112}$$

and load-shortening

$$\Delta P = S_\varepsilon \Delta\varepsilon \tag{113}$$

where per definition the postbuckling coefficients S_κ and S_ε are

$$S_\kappa = \frac{K_{11}}{K_{21}}\left(\frac{P_C}{P_E}(EI_T) - K_{22}\right) + K_{12} \tag{114}$$

$$S_\varepsilon = K_{11} + \frac{K_{12}K_{21}}{(P_C/P_E)(EI_T) - K_{22}} \tag{115}$$

Substituting the macro material solution, i.e. Eq. (109) into Eq.(114) and into Eq.(115), this gives for the coupled local-overall postbuckling coefficients the following expressions

$$S_\kappa = \left[\frac{8\sqrt{3}}{15}\left(\frac{P_C}{P_E} - \frac{7}{12}\right) - \frac{5\sqrt{3}}{18}\right]\sqrt{(EA_T)(EI_T)} \tag{116}$$

$$S_\varepsilon = \left[\frac{4}{9} + \frac{(25/108)}{(P_C/P_E) - (7/12)}\right](EA_T) \tag{117}$$

These solutions are discussed for two extreme cases as follows. First the most severe case of coincident buckling is analysed, i.e. requiring

$$P_C = P_E \tag{118}$$

Substituting Eq.(118) into Eq.(116),(117) gives

$$S_\kappa = -\frac{\sqrt{3}}{18}\sqrt{(EA_T)(EI_T)} \tag{119}$$

$$S_\varepsilon = (EA_T) \qquad \text{max. snap back} \tag{120}$$

From Section 2.4 it follows that snap-back behaviour will be present if $\infty > S_\varepsilon > (EA_T)$. Eq.(120) gives S_ε to be equal to full cross-sectional axial stiffness EA_T. This means that the

postbuckling response is extremely unstable with a snap-back equilibrium path tangential to the linear stiffness prebuckling path at P_C.

From Eq.(117) it can be conclude that if $P_C/P_E > (7/12)$ there will always be snap-back behaviour. In the limit $P_C/P_E = (7/12)$ neither negative nor positive axial stiffness is found, i.e. the loads drops down at an infinite rate at P_C with respect to the axial shortening ε.

Another extreme case for discussion is that of

$$P_E >> P_C \tag{121}$$

Under this condition, Eq.(116) and Eq.(117) becomes

$$S_\kappa = -\frac{53\sqrt{3}}{45}\sqrt{(EA_T)(EI_T)} \tag{122}$$

$$S_\varepsilon \equiv \frac{1}{21}(EA_T) \tag{123}$$

It is interesting to observe that the solution of Eq.(123) is exactly the same as given by Rhodes (1982). This solution predicts almost zero axial stiffness ($1/21 \approx 0.05$) when local buckling starts in a stiffener with a long span. This low value has to seen in connection with the main assumption for how the external load P acts in the present Shanley model, i.e. it always acts in the centroid of the cross-section.

As a final verification of the closed form solution, the reduced modulus factor, given by Eq.(40) for a general section shape, is evaluated. Substituting Eq.(109) into Eq.(40) gives simply

$$\eta_{BR} = \frac{1}{16} \tag{124}$$

This is also exactly the same value as calculated by Rhodes (1982) using a different approach.

As a final comment on the presented solution for the coupled local and overall response, it is emphasised that the external load P always acts in the centroid of the cross-section. This is a basic assumption for the present section results, but it affects not the pure macro model solutions developed in Chapter 4.

The general section Shanley model was basically constructed with the purpose of throwing some light into the non-linear interactive buckling of stiffened panels. It is not a problem to extend the model to also cover a continuously moving external load case, as will be most realistic for continuous stiffened panels in ship structures. However, this type of extensions have to be seen in relation to other types of loading acting typically bi-axial loading, in-plane shear, lateral pressure etc. These are all topics that have to be included in complete semi-theoretical buckling model for stiffened panels.

5.3.3 Numerical solution - Flat bar profile in tanker deck

The numerical buckling model, with an implemented incremental perturbation scheme and automatic arc length control, has been programmed on a personal computer and tested on two examples.

The first example is a stiffened panel of an oil tanker with a displacement of 130 000 tons has been chosen. The structural layout for the deck consists of a flat bar profile welded to the plating with an equal spacing s. The geometrical proportions and material characteristics are given in Table 5.2.

Data parameters	Tanker deck – Flat bar
t_p [mm]	18
s [mm]	910
t_w [mm]	20
h_w [mm]	325
t_f [mm]	0
b_f [mm]	0
L [mm]	4750
E [N/mm^2] Young's modulus	208 000
ν Poisson ratio	0.3
σ_F [N/mm^2] Yield stress	355

Table 5.2 Geometrical proportions and material parameters.
Deck panel in a 130 000 tons tanker.

It should be noted that the yield stress have no physical implications for the results presented in this section. The material yield stress σ_F is only used for scaling purposes in the numerical scheme and in the figures presented.

The present model gives the following values for the ideal elastic local buckling stresses (eigenvalue in mode q_1, Chapter 4 and Appendix 5)

$$\sigma_C = \mathbf{315}\ \text{MPa} \qquad \text{Torsional buckling mode}$$

The overall elastic column buckling stress is (Euler load Eq.(15) excluding all local cross-sectional effects)

$$\sigma_E = \mathbf{772}\ \text{MPa} \qquad \text{Euler buckling mode}$$

These eigenvalues shows, as expected for typical ship deck profiles that the local buckling stress σ_C is significantly lower than the overall column buckling stress σ_E.

The initial stiffness postbuckling coefficient S_ε, as defined in Eq.(115), includes the coupling effect between local torsional buckling and overall column buckling. For the present example it is found to be

$$S_\varepsilon = \mathbf{0.334}\, EA_T \qquad \text{Overall in-plane stiffness}$$

This means that when the stiffened panel buckles at the local torsional buckling stress of **315** MPa it will have an axial stiffness of **33** % of the full axial stiffness when further compressed into the postbuckling region.

The reduced modulus factor is calculated to be **0.93** which means that the nominal reduced modulus stress is σ_R = **0.93*772,** i.e.

$$\sigma_R = \mathbf{718}\ \text{MPa} \qquad \text{Reduced modulus stress}$$

These calculated parameters describe the onset of local buckling, initial and advanced postbuckling characteristics of a geometrically perfect version of the present stiffened panel. A simple interpretation of these parameters gives the following load-shortening characteristic:

Elastic buckling starts with the onset of a local torsional/sideways stiffener mode interacting with plate buckling between stiffeners at a nominal stress of **315** MPa. The local buckling mode will immediately trigger an interaction with the overall column buckling mode and the initial axial stiffness of the panel is **33 %** of the full stiffness when compressed beyond **315** MPa. In the advanced postbuckling region, the axial stiffness will gradually drop and approach zero for an axial nominal stress of **718** MPa.

In order to study the behaviour of a geometrically imperfect panel, the imperfection amplitudes both in the local q_1 mode and overall column mode ξ have been varied systematically. Results are presented in the following figures. Note that that notation ξ represent the parameter κ in the Shanley model, i.e. the only difference is that ξ is an non-dimensional parameter and it is defined as the overall lateral displacement scaled with the plate thickness t_p. The corresponding overall geometrical imperfection is given the symbol ξ_0. The torsional/sideways imperfection q_{10s} indicates the sideways tilt (non-dimensional with thickness t_w) of the stiffener (measured at the top of the free stiffener end).

Fig.14 shows the result for the case where the local stiffener and plate imperfection are kept constant at a low value, i.e. sideways stiffener tilt is $q_{10s} * t_w$ = 1 mm, which in the present model is consistent with a plate imperfection $q_{10p} * t_p$ = 0.9 mm. The overall Euler imperfection amplitude $\xi_0 * t_p$ is varied between 1 and 20 mm. In Fig. 14 (and the following Figs.15, 16, 17) the horizonal axis represent a non-dimensional axial shortening of the cross-section centroid symbolised as $u/u_F = \varepsilon/\varepsilon_F$. The vertical axis represents a non-dimensional

axial load $P / P_F = \sigma_x / \sigma_F$. P_F is the squash load defined as $P_F = \sigma_F * A_T$. The corresponding squash shortening u_F is defined as $u_F = (\sigma_F/E)*L$.

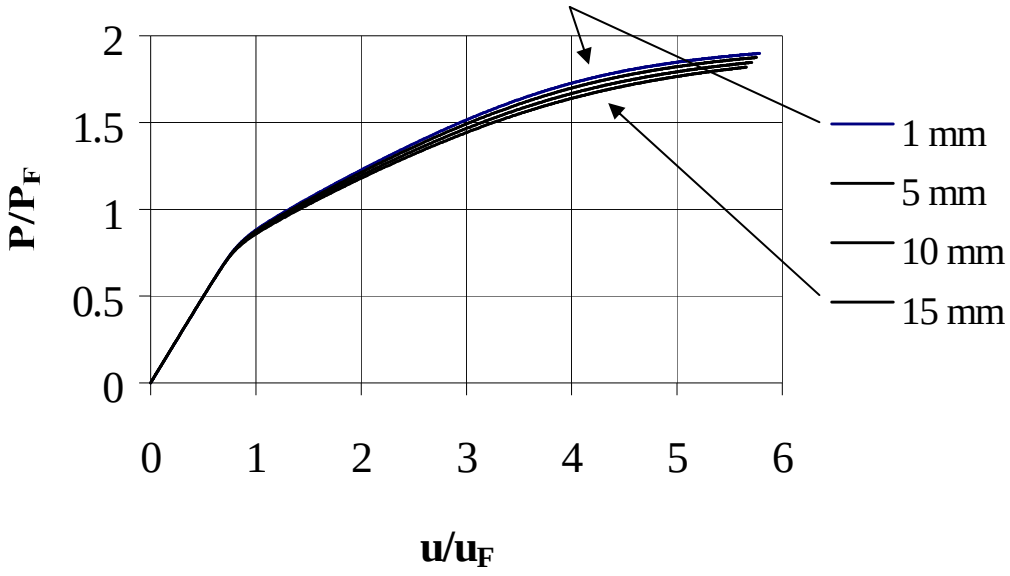

Fig.14 Load-shortening curves for a stiffened panel with flat bar stiffeners with almost perfect cross-sectional shape. Sideways tilt of stiffener top kept fixed at 1 mm, the overall column imperfection amplitude $\xi_0 * t_p$ is varied between 1 to 15 mm

It is seen from Fig.14 that the geometrical imperfection in the overall column Euler mode do not have any pronounced effect on the load-shortening characteristic until the advanced postbuckling region is reached. In the advanced postbuckling region, the axial stiffness decreases continuously and approaches zero at value of P/P_F of approximate 2.0. (718/355 = 2.0 is the scaled reduced modulus load).

In Fig.15 the overall stiffener imperfection is kept constant at a low level, i.e. $\xi_0 * t_p = 1$ mm while the sideways stiffener imperfection amplitude $q_{10s} * t_w$ is varied between 1 and 20 mm (associated plate imperfection q_{10p} = 0.9 to 18 mm).

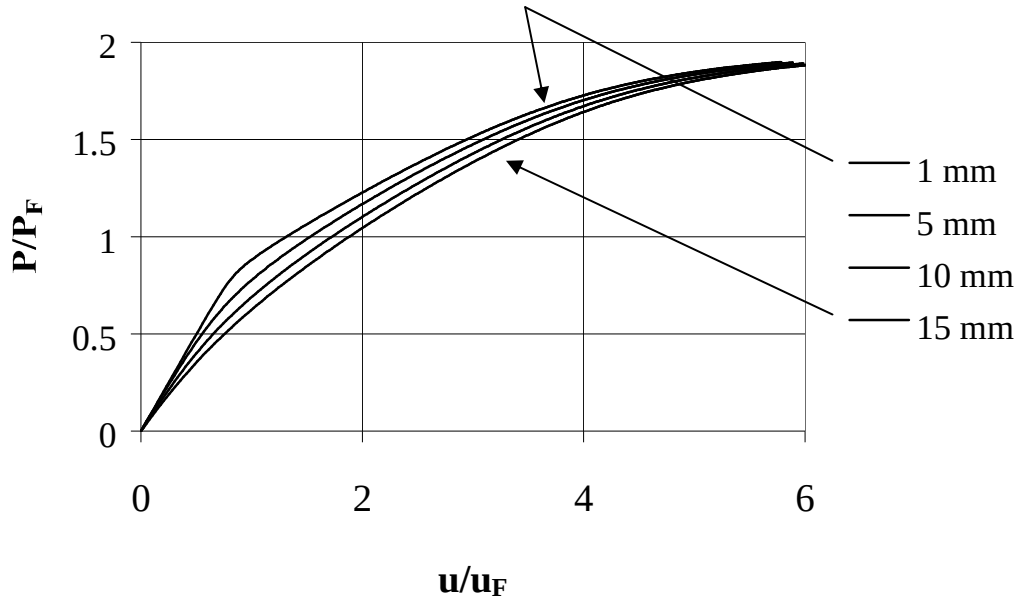

Fig.15 Load-shortening curves for a stiffened panel with flat bar stiffener with variable geometrical imperfections in the cross-section and almost perfect straight column axis.
Sideways stiffener tilt at top varied between 1 to 15 mm and the overall imperfection amplitude $\xi_0 * t_p$ is kept fixed at 1 mm

Fig. 15 reveals that the geometrical imperfections in the cross-section of the panel have a much more pronounced effect on the load-shortening characteristic than the out-of straightness of the column axis shown in Fig.14. It is clearly seen that the in-plane stiffness is much below the full linear stiffness already from the very start of loading. The highest rate of axial stiffness reductions is in the region of the local critical buckling stress **315** MPa. In the advanced postbuckling region the effect of the local imperfections is reduced and the equilibrium curves for different imperfection levels approach each other.

If these results are related to normal shipyard standards it can be expected that the axial stiffness of such panels be significantly reduced compared to the full linear stiffness values. Normal shipyard standard for the present oil tanker will give out-of-flatness of the order of 5-10 mm in the plating between stiffeners. Out-of-straightness tilt of flat bar stiffeners is not that well documented, but can be estimated to be of the order of 10 mm. This may give typical axial stiffness reductions of the order 10-20% as a reasonable estimate for deck designs of tankers. It is added as a comment that the present analysis always takes the geometrical imperfections to coincide with minimum the eigenmodes as a conservative approach. Actual imperfections in welded ship decks will have a complex and random pattern. This fact makes the picture more complicated, but does not violate the qualitatively buckling and postbuckling results presented here.

5.3.4 Numerical solution - Coincident overall and local buckling

As an alternative example, a stiffened panel is constructed with the purpose of illustrating unstable postbuckling behaviour. Unstable postbuckling response will typically occur for panel designs where the local and overall column Euler buckling eigenvalues are close. In order to construct such an example the cross-sectional form of a ship bottom panel was used, but the stiffener span was increased significantly compared what is normally found.

Data parameters	Constructed case – T profile
t_p [mm]	13
s [mm]	910
t_w [mm]	24.5
h_w [mm]	400
t_f [mm]	19
b_f [mm]	90
L [mm]	12000
E [N/mm^2] Young's modulus	208 000
ν Poisson ratio	0.3
σ_F [N/mm^2] Yield stress	355

Table 5.3 Geometrical proportions and material parameters used in a constructed example illustrating unstable coupled local and overall buckling.

The present model gives the following values for the local ideal elastic buckling stresses (eigenvalues)

$\sigma_C = \mathbf{313}$ MPa q_1 torsional mode

$\sigma_C = \mathbf{620}$ MPa q_2 web mode

The overall column Euler buckling stress, excluding local cross-sectional effects, is

$\sigma_E = \mathbf{320}$ MPa Euler buckling mode

The low overall elastic buckling stress of **320** MPa is due to the very long stiffener span of 12 meter.

As for the previous example the axial stiffness parameter S_ε is assessed and found to be

$S_\varepsilon = \mathbf{1.05}\, EA_T$ Overall axial stiffness

This means that we have a panel design showing snap-back buckling response and is thus extremely initially unstable when entering the postbuckling region.

The reduced modulus factor is calculated to be **0.43** which means that the nominal reduced modulus buckling stress is σ_R = **0.43*320**, i.e.

σ_R = **137** MPa Reduced modulus stress

These parameters, valid for a geometrically perfect panel, then predict a severe unstable elastic buckling response as summarised as follows:

The buckling will start at a uniform membrane stress of **313** MPa and is associated with a torsional sideways buckling of the stiffener. The local buckling will immediately trigger a coupling with the overall column buckling mode, leading to an initial snap-back behaviour. The snap-back behaviour means that axial stiffness is no longer available i.e. in order to trace the equilibrium path, not only the load P, but also the end-shortening u will initially decrease. The unstable equilibrium path will then twist and the axial shortening u will start to increase again while the load continues to drop. The nominal stress will then asymptotically approach the reduced modulus stress of **137** MPa in the advanced postbuckling region.

As for the previous numerical example, load-shortening curves are generated for different levels of geometrical imperfections. The results are shown in the following figures, Fig.16 and Fig.17 respectively.

Fig.16 shows the result for the case where the local stiffener and plate imperfection are kept constant at a low value, i.e. sideways stiffener tilt of the stiffener top is $q_{10s} * t_w$ = 1 mm which in the present model is consistent with a plate imperfection of $q_{10p} * t_p$ = 0.7 mm. The overall column imperfection $\xi_0 * t_p$ amplitude is varied between 1 and 20 mm.

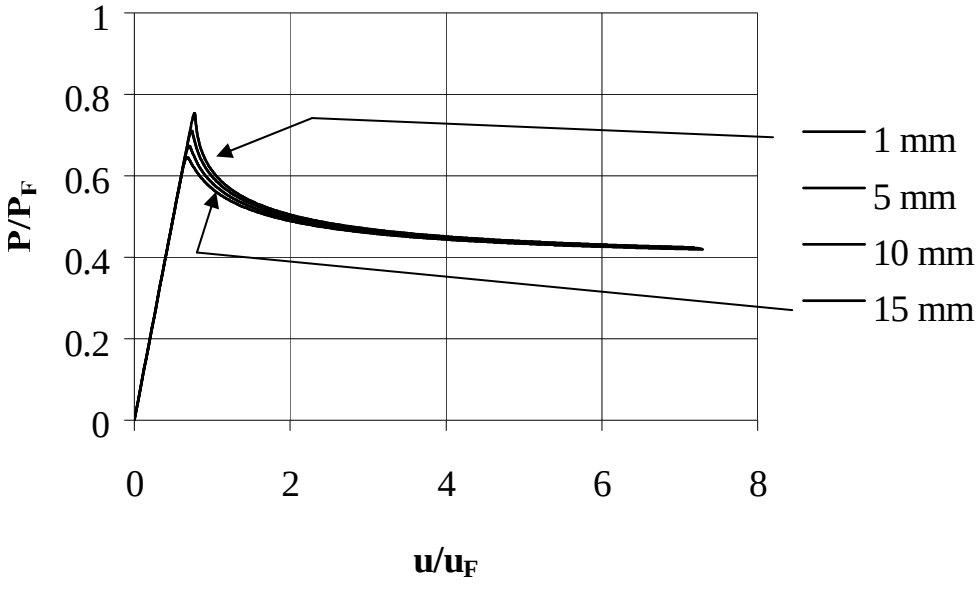

Fig.16 Load-shortening curves for a panel with near coincident local and overall eigenvalues. Almost perfect cross-sectional shape with variable overall imperfection amplitude $\xi_0 * t_p$ between 1 to 20 mm

From Fig. 16 it is seen that the geometrical imperfection in the overall column mode have a pronounced effect on the limit load (ultimate strength) while it have no influence on the axial stiffness properties before the ultimate load is reached. In the advanced postbuckling region the load approach the reduced modulus load and the overall imperfection effect in this region is of no significance.

In Fig.17 the overall stiffener imperfection is kept constant at a low level, i.e. $\xi_0 * t_p$ = 1 mm while the sideways stiffener imperfection amplitude $q_{10s} * t_w$ is varied between 1 and 20 mm (associated plate imperfection between stiffeners $q_{10p} * t_p$ = 0.9 to 18 mm).

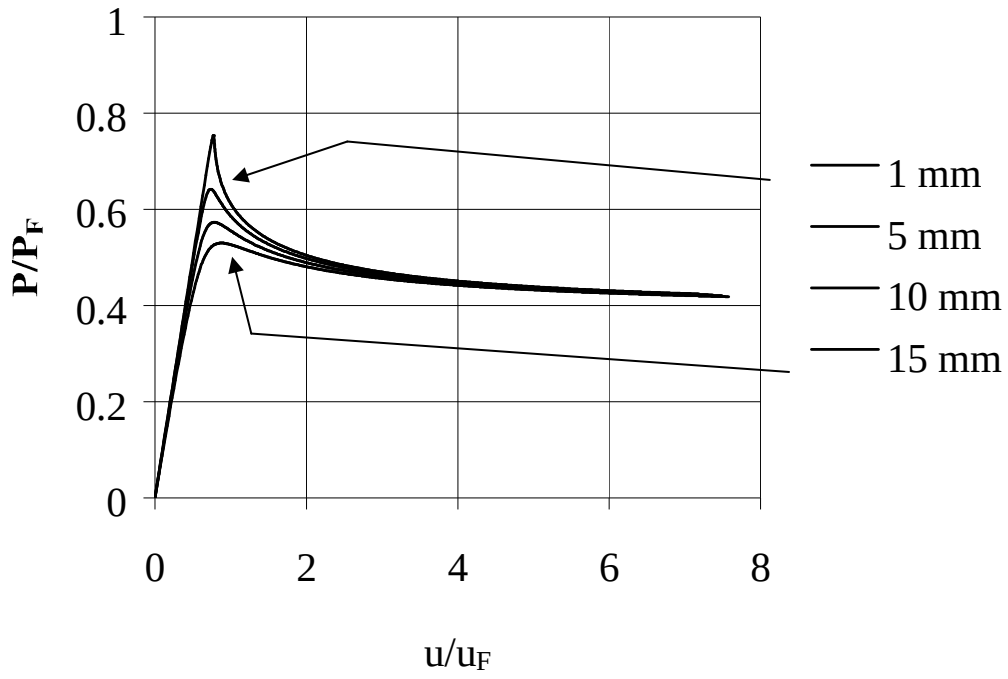

Fig.17 Load-shortening curves for a panel with near coincident local and overall eigenvalues. Variable local imperfections in cross-section, range 1 to 20 mm. The column axis is almost perfect assuming a max amplitude $\xi_0 * t_p$ of 1 mm

From Fig. 17 it is seen that the geometrical imperfection in the form of local sideways tilting of the stiffener have a pronounced effect on the limit load (ultimate strength) while it have marginal influence on the axial stiffness. In the advanced postbuckling region the load approach the reduced modulus load and the imperfection effects in this region vanished.

It is found for this example that the severe non-linear coupling between local and overall buckling modes reduce the ultimate buckling capacity to only **176** MPa compared to the strength of the geometrically perfect panel of **313** MPa. This 44 % knock down effect is assessed for a sideways initial tilt at the free stiffener edge of 20 mm which is slightly less than the stiffener web thickness of 24.5 mm

This example demonstrates the severe imperfection sensitivity, with respect to ultimate buckling capacity, stiffened plates may experience when they are designed with close or coincident local and overall eigenvalues. The local imperfections are seen to be most influential on the ultimate stress, but also the overall imperfections have a significant knock down effect. As for the previous example the axial stiffness before ultimate stress is mostly affected by the presence of local cross-sectional imperfections, but to a less degree. Out-of straightness of the column axis influences the axial stiffness properties only marginally.

5.4 Summary and discussion

The present chapter presents some general closed form solutions and two numerical examples applying the present theoretical model. Some limited comparisons with solutions found in the literature are given. The verification is split in two parts, the first part is given in Section 5.2 and is exclusively devoted to the macro model developed in Chapter 4. Section 5.3 is devoted exclusively to coupled local and overall buckling.

Section 5.2 and Section 5.3 presents some closed form solutions for the present macro model assuming single mode buckling response. Comparisons are given with some analytical solutions found in the literature. In Section 5.2 some numerical results for reduced modulus factor for slender stiffeners found in the literature is given. Excellent agreement with the present model was found.

In Section 5.3 two numerical examples using the present model was presented. The first example has typical dimensions as for stiffened panels in large steel ships. The second example was constructed in order to illustrate the unstable response typical for panels with close local and overall eigenvalue. These examples were generated using the present developed incremental perturbation scheme with arc length control.

The two numerical examples illustrate some typical features of non-linear buckling response of stiffened panels in the geometrical non-linear range. By varying the imperfection amplitudes in the local and overall mode separately, important information as to the strength and stiffness characteristics of stiffened panels is uncovered.

6. SUMMARY AND CONCLUSION

The main motivation for the present work has been to gain insight into the mechanics of geometrically non-linear interactive buckling between local and overall buckling modes in stiffened panels. Based on such insight it will be possible to develop useful concepts, which can be used in semi-theoretical computerised buckling models for the strength and stiffness estimates of such panels.

The present buckling model has two separate parts. The first part deals exclusively with the cross-sectional macro material model and the second part, here using the general section Shanley model, couples the macro material model to the overall column buckling.

Special efforts have been given to a development of a macro material model, relevant for stiffened panels with open profiles as found in ship and offshore constructions. This macro model is two-dimensional. This means that it is suited for application to panels exclusively subjected to axial loading. For combined loading, such as in-plane bi-axial loading and in-plane shear, a six-dimensional model is needed. This problem is touched upon, but not addressed in detail here. Further, the present macro material model is approximated as two-degree of freedom model, covering torsional/sideways buckling of stiffeners interacting with a plate buckling (q_1 mode) and stiffener web buckling also interacting with a plate buckling (q_2 mode). It is emphasised that the present two-degree of freedom model gives a very crude simplification of real structural response, but the model is thought to be relevant for a wide range of stiffened panels encountered in ship steel and aluminium constructions. Naturally, the present macro model could be further improved by adding more degrees of freedom for accurate strength and stiffness estimates. In fact the macro model concept as developed herein, is equally applicable for many local degrees of freedom (local displacement vector q_i) as for few. This makes the model flexible for later extensions. More work in this area is needed both with respect to theoretical development of multi-dimensional macro models and with respect to verification with other general purpose non-linear finite element codes such as ABAQUS (1998). The present report does not include verifications against such advanced programs, but includes verification rather on the more conceptual level. In particular can be mentioned verifications against other analytical closed formed solutions as well as comparisons against some limited numerical results for reduced stiffness parameters, all found in the literature.

Another feature of the present work is that it is built on the general non-linear stability theory, developed in a discrete finite-dimensional form by Sewell, Thompson, Huseyin and others in the seventies in UK. They introduced the perturbation method as a numerical strategy for solving sets of non-linear algebraic equations and for studying bifurcations and postbuckling behaviour of complex plate and shell problems. This approach has been used herein, however, extended for use in an incremental scheme for tracing continuous equilibrium paths, much in the same way as done in standard non-linear finite element programs. By using an arc length control, it has been demonstrated on two examples that the present approach is capable of tracing continuous equilibrium paths with limit points, snap-back behaviour and severe imperfection sensitivity. More about this numerical scheme can be found Steen(1998).

As a final comment it is emphasised that the present work is mainly devoted to the development of simplified buckling models and concepts, at the expense of detailed numerical verifications using alternative methods. This has been the strategy selected due to personal preferences and supported by the belief that simple models can be used for the construction of computerised, fast buckling models. Such models will provide more information and predict more realistic strength estimates than current available rules and codes. By reviewing the literature on buckling of stiffened plates it is observed that most of it is dedicated to advanced numerical studies using different types of standard finite element programs or similar software. It is thought that the development of simple and physical models like the present is more important for gaining understanding of the buckling phenomena themselves, and this subject has not had the attention it deserves in the literature during the last two decades. Thus, by ensuring a more proper balance in the future, between the development of physical semi-theoretical models like the present, and full blown numerical finite element studies, it is believed that safe and optimal buckling design procedures are in the hands of designers and authorities within a relatively short time.

Acknowledgements

Without the continuous support from dr. S.Valsgård and G.Holtsmark, DNV, and professor J.Hellesland, University of Oslo, this project would never have landed and their interest and encouragement has been of vital importance. Patient assistance by my colleagues Eirik Andreassen, Gaute Storhaug and Anders B. Engelsen at DNV is also highly appreciated. Thanks also to drs. Geir Skeie and Ole Chr. Astrup at DNV for helping in verification some of the theoretical basis for the present numerical model. Thanks also to drs. B. Hayman and S. Gran, DNV, for their support in the initial phase of the present project. A special salute goes to Tom K. Østvold, DNV for his dedicated interest in the present subject and continuous encouragement. Finally I wish to thank DNV represented by O.P. Torset and R. Løseth for their important backing and financial support.

7. REFERENCES

ABAQUS, Version 5.8, User's Manual, Hibbitt, Karlsson & Sorensen, Inc. 1998.

ABAQUS (1996), "Analysis of Composite Materials with ABAQUS", Hibbitt, Karlsson & Sorensen, Inc. 1998.

Ayrton, W.E and Perry, J. (1886). "On struts", The Engineer, **62**. 464-465, 513-515.

Bangstein. B.H. (1994). "Knekning av Platebærere", Thesis in Mechanics, Presented for the degree of Cand. Scient, University of OSLO, Department of Mathematics, Division of Mechanics, May 1994. (in Norwegian)

Bobb. A.(1994). "Buckling of Stiffened Plates - Numerical Analysis using ANSYS", Thesis in Mechanics, Presented for the degree of Cand. Scient, University of OSLO, Department of Mathematics, Division of Mechanics, June 1994.

Brush, D.O. and Almroth, B.O. (1975) " Buckling of Bars, Plates, and Shells". McGraw-Hill, International student edition.

Budiansky, B. and Hutchinson, J.W. (1979). " Buckling: Progress and Challenge ". Trends in Solid Mechanics, Proceedings of the Symposium dedicated to the 65th Birthday of W.T. Koiter, Delft University June 1979, Editors: Besseling, J.F. and van der Heijden A.M.A. Delft University Press, Sijhoff & Noordhoff International Publishers.

Campus, F.and Massonnet, C. "Colloque sur le comportement postcritique des plaques utilisees en construction metallique". Interventions de W.T.Koiter et M.Skaloud, pp.64-68, 103,104. Memoires de la Societe Royale des Sciences de Liege, 5-me serie, tome VIII, fsc. 5 (1963).

Chilver A.H. and Britvec, S.J. (1964). "The plastic buckling of aluminium columns". Proc. Symp. Aluminium in Structural Engineering, Aluminium Federation.

Croll, J.G.A. and Walker A.C. (1972). "Elements of Structural Stability", Macmillan Press Ltd., London and Basingstoke.

Dym, J.L. (1974). "Stability Theory and its Application to Structural Mechanics", Nordhoff, Leyden, The Netherlands.

Ellinas, C.P., Kaoulla, P., Kattura, S. and Croll, J.G.A. (1977). "Tests on Interactive Buckling of Stiffened Plates". Experimental Mechanics, **17**, pp.455-462.

Ellinas, C.P. and Croll, J.G.A. (1979). "The Basis of a Design Approach for Stiffened Plates". Stability Problems in Engineering Structures and Components. Eds. Richards, T.H. and Stanley, P.

Ellinas, C.P. and Croll, J.G.A. (1981). "Post-Critical Analysis of Torsionally Buckled Stiffener Plates". Int.J.Solids Structures,**17**, pp.11-27.

Fung, Y.C. (1965) "Foundations of Solid Mechanics", Prentice-Hall, Inc.

Graves Smith, T.R. (1967). "The Ultimate Strength of Locally Buckled Columns of Arbitrary Length". Thin Walled Steel Constructions. Ed. Rockey and Hill. London: Crosby Lockwood .

Graves Smith, T.R. (1968). "The Post-buckled Strength of Thin Walled Columns". IABSE conf. New York.

Huseyin, K. (1975)."Nonlinear theory of elastic stability", Noordhoff International Publishing, Leyden.

Hutchinson, J.W. (1974). " Plastic Buckling". Advances in Applied Mechanics, Vol.14. Acedemic Press.

Koiter, W.T. (1945). "On The Stability of Elastic Equilibrium (in Dutch with English summary)", Thesis, Delft, H.J. Paris, Amsterdam, 1945. English translation: Air Force Flight Dyn.Lab.Tech.Rep.AFFDL-TR-70-25, 1970.

Koiter, W.T. (1963). "Introduction to the post-buckling behaviour of flat plates". Memoires in -8° de la Societe Royale de Sciences de Liege, 5^{me} serie, Tome VIII, Fascicule 5, pp.17-40.

Koiter, W.T. and Kuiken, G.D.C. (1971). "The Interaction Between Local Buckling and Overall Buckling on the Behaviour of Built-up Columns". WTHD Report 23, Delft.

Marguerre, K. (1938). "Zur Theorie der gekrümmten Platte grosser Formändrung", Proceedings of the 5th International Congress for Applied Mechanics, pp.93-101.

Rhodes, J. (1982). "Effective Widths in Plate Buckling". Developments in Thin-Walled Structures-1. Ed. Rhodes, J. and Walker, A.C., Applied Science Publishers, London.

Robertson A.(1925), Institution of Civil Engineers, Selected Engineering Papers No.28.

Shanley, F.R. (1947). "Inelastic Column theory", J. Aeronautical Sci., Vol. 14, pp. 261-267.

Smith, C.S. (1975). "Compressive strength of welded steel ships grillages". Trans. RINA, Vol.117, pp.325-359.

Smith, C.S. (1990). "Design of Marine structures in Composite Materials". Elsevier Applied Science.

Steen, E, (1989). "Elastic Buckling and Postbuckling of Eccentrically Stiffened Plates", Int.J.Solids and Structures, Vol. 25.

Steen, E. (1998). "Application of the Perturbation Method to Plate Buckling Problems". University of Oslo, Department of Mathematics, Mechanics Division, Report No. 98-1, ISSN 0801-9940, ISBN 82-553-1149-1.

Steen, E and Andreassen, E. (1995-I). “Buckling of Stiffened Plates under Combined Loads. PP2: Basic Theory Development CSA-2”, DNV Report No.95-0198.

Steen, E and Andreassen,E. (1995-II). “Buckling of Stiffened Plates under Combined Loads. PP2: Detailed Theory Development CSA-2”, DNV Report No.95-0479.

Stowell, E.Z. (1951). “Compressive Strength of Flanges”, NACA Tech. Rep. No.1029.

Timoshenko, S. and Woinowsky-Krieger, S. “Theory of Plates aand Shells”, McGraw-Hill, International Studendt Edition.

Thompson, J.M.T. and Lewis,G.M.. (1972). “On the Optimum Design of Thin-Walled Compression Members”. J.Mech.Phys. Solids **20**, 101-109.

Thompson, J.M.T. and Hunt, G.W. (1973). “A general theory of elastic stability”, John Wiley & Sons, Great Britain.

Thompson, J.M.T., Tulk, J.D. and Walker A.C. (1974). “An Experimental Study of Imperfection Sensitivity in the Interactive Buckling of Stiffened Plates”. Buckling of Structures, Symposium Cambridge/USA, Editor. B.Budiansky, Springer-Verlag, Berlin Heidelberg New York 1976.

Tulk, J.D. and Walker, A.C. (1976). “Model Studies of the Elastic Buckling of a Stiffened Plate”. Journal of Strain Analysis, **11**, No.3.

Tvergaard,V. (1973). “Imperfection Sensitivity of a Wide Integrally Stiffened Panel under Compresssion”. Int.J.Solids and Structures, **9**, pp.177-192.

Tvergaard,V. and Needleman A. (1975) “On the Buckling of Elasto-Plastic Columns with Asymmetric Cross-sections”. Int.J. Mechanics. Sci. Vol.17.

Van der Neut, A. (1969). “The Interaction of Local Buckling and Column Failure of Thin Walled Compression Members”. Proc. 12th Int. Congr. Appl. Mech. Stanford University (1968). Berlin, Heidelberg, New York, Springer, pp.389-399.

Von Karman, T. (1910). Forschungsarb. No. 81, Berlin

Walker, A.C. (1975). “Interactive buckling of structural components”, Sci. Progr.,**62**, pp.579-597.

8. NOTATION

Latin letters

a,b,c	These letters with Latin numbers as subscripts define constants in the potential energy function V in the local cross-sectional mode, Appendix A1
c_f	Distance from cross-sectional centroid to stiffener flange middle plane
A	General symbol for cross-sectional area
A_T	Total cross sectional area of column unit cross-section, $A_T = (s\, t_p + h_w\, t_w + b_f\, t_f)$
b_f	Stiffener flange width (total width)
B_{11}	Parameter, defined in Appendix A6
B_{12}	Parameter, defined in Appendix A6
B_{21}	Parameter, defined in Appendix A6
B_{22}	Parameter, defined in Appendix A6
D	Stability determinant, local modes $D = \left\|V_{ij}\right\|$
e_f	Eccentricity of stiffener flange centroid relative to stiffener middle stiffener web plane
E	Young's modulus
EI_T	Bending stiffness of column
EA_T	Axial stiffness of column
g	This letters with number 1 or 2 and letter u or θ as subscripts defines constants in the potential energy function V in the local cross-sectional mode, Appendix A1
h_w	Stiffener web height (exclusive flange thickness)
H	Mean section height parameter, $H = (t_p + t_f)/2 + h_w$)
I_0	Symbol for the unloaded state
I_C	Symbol for the local critical state, perfect geometry, buckling into mode q_1 or q_2
I_s	Symbol for any loaded state
I_T	Moment of inertia of cross-section about centroid per unit width (about $z = z_G$)
I_f	Moment of inertia of stiffener flange ($I_f = \frac{1}{12} b_f^{\,3} t_f + e_f^{\,2} \frac{b_f t_f}{(1 + b_f t_f / (h_w t_w))^2}$)
J_p	Torsional stiffness of stiffener flange ($J_p = \frac{1}{3} b_f t_f^{\,3}$)
K_{11} K_{12} K_{21} K_{22}	Macro tangent stiffness coefficients of a general cross-section evaluated at any state I_s .
$K_{11}^{\,L}$ $K_{12}^{\,L}$ $K_{21}^{\,L}$ $K_{22}^{\,L}$	Linear elastic stiffness coefficients for column unit cross-section
L	Length of continous Euler column, full stiffener span for panels
L_ε	Load parameter in local mode, single degree of freedom model, Appendix A3
L_κ	Load parameter in local mode, single degree of freedom model, Appendix A3

M	Total internal moment in column unit about centroid z_G at mid-length of column, stiffener + plate unit with unit width s, positive give compression for $z > z_G$ in stiffener
M_F	Scaling first yield moment, $M_F = EI_T \theta_F/L$
N	Total internal axial load in column unit, stiffener + plate unit with unit width s, positive in compression
p	Number of half waves in x-direction in web q_2 mode
P	External axial load, positive in compression
P_E	Euler buckling load for perfect stiffener/plate column unit, width s
P_C	Local buckling load for perfect stiffener/plate column unit, width s, mode q_1 or q_2
P_R	Reduced modulus load of column unit, $P_{RM} \equiv \eta_{RM} P_E$
P_M	Limit point load from Koiter theory of Shanley column model
P_F	Squash load of column unit, $P_F \equiv \sigma_F A_T$
P_U	Ultimate load capacity of column unit
q_i	General displacement vector for local cross-sectional modes in macro model, non-dimensionless
q_{i0}	General displacement vector for initial stress free imperfections in cross-section, non-dimensionless
q_{1s}	Dimensionless sideways deflection amplitude of stiffener top, Eq. (64), Fig.11a
q_{10s}	Dimensionless initial sideways deflection amplitude of stiffener top
q_{1p}	Dimensionless deflection of plate, torsional stiffener-plate mode, Eq.(65), Fig.11a
q_{10p}	Dimensionless initial deflection of plate, torsional stiffener-plate mode
q_{2s}	Dimensionless deflection amplitude at stiffener web mid height, Eq.(64), Fig.11b
q_{20s}	Dimensionless initial deflection amplitude at stiffener web mid height
q_{2p}	Dimensionless deflection of plate, stiffener web-plate mode, Eq.(65), Fig.11b
q_{20p}	Dimensionless initial deflection of plate, stiffener web-plate mode
q_1	Short notation, $q_1 \equiv q_{1s}$
q_{10}	Short notation, $q_{10} \equiv q_{10s}$
q_2	Short notation, $q_2 \equiv q_{2s}$
q_{20}	Short notation, $q_{20} \equiv q_{20s}$
q	Number of half waves in x-direction in torsional q_1 mode
R_1	Parameter ($R_1 \equiv \frac{t_w}{t_p}\frac{s}{H}\frac{1}{\pi}$), Eq.(69)
R_2	Parameter ($R_{21} \equiv \frac{t_w}{t_p}\frac{s}{H}$), Eq.(69)
s	Stiffener spacing, unit width of column model
S_κ	Initial postbuckling coefficient, slope of load-curvature relation
S_ε	Initial postbuckling coefficient, slope of load-shortening relation (axial stiffness)
t_p	Plate thickness
t_w	Stiffener web thickness
t_f	Stiffener flange thickness
u_α	In-plane deflection of plate in x_α direction, general notation
u_1	In-plane deflection of plate in x_1 direction, general notation
u_2	In-plane deflection of plate in x_2 direction, general notation
u_G	Relative end-shortening of column cross-section centroid, positive in compression

u	Relative end-shortening of column cross-section centroid, $u \equiv u_G$ in Figs.14,15,16,17 for convenience
$\bar{u}$	Relative end-shortening of column edges in any point along stiffener height, $\bar{u} = u = u_G$ for $z = z_G$
u_F	Squash axial shortening, $u_F = \varepsilon_F L$
V	Potential energy per unit volume ($A_T L$), Appendix A1
V_{unit}	Potential energy per unit
w	Plate deflection normal to plate plane, general notation for component plate
w_0	Initial plate deflection normal to plate plane (stress free initial imperfection)
w_s	Local sideways deflection of stiffener web plate (deflection in y direction, i.e. normal to web plane)
w_{s0}	Local sideways initial deflection of stiffener web plate (deflection in y direction, i.e. normal to web plane)
w_p	Local deflection of plate between stiffeners (deflection in z direction, i.e. normal to plate plane exclusive overall column deflection)
w_{p0}	Local initial deflection of plate between stiffeners (deflection in z direction, i.e. normal to plate plane exclusive overall column deflection)
w_ξ	Overall deflection amplitude of continous Euler column and Shanley column, $w_\xi = \theta \bar{L} = \kappa L\bar{L}$
$w_{\xi 0}$	Overall deflection amplitude of continous Euler column and Shanley column, $w_{\xi 0} = \theta_0 \bar{L} = \kappa_0 L\bar{L}$
x	Co-ordinate in for macro model in stiffener direction, laying in plate middle plane
y	Co-ordinate in for macro model in transverse direction, laying in plate middle plane
z	Co-ordinate for macro model along stiffener web height, laying in stiffener web middle plane, centroid $z = z_G$ see Fig.10
X	Co-ordinate in Shanley model, laying in centroid of cross-section directed along column axis, Fig.3
Y	Co-ordinate in Shanley model column cross-section, see Fig.3
Z	Co-ordinate in Shanley model column cross-section, see Fig.3
x_α	General cartesian in-plane co-ordinate, $\alpha = 1, 2$
x_1	Cartesian in-plane co-ordinate
x_2	Cartesian in-plane co-ordinate
x_3	Cartesian co-ordinate perpendicular to plate plane
z_G	Centroid of macro model unit; stiffener with full plate width s, z co-ordinate measured from plate middle plane, Fig.10.

Greek symbols

Δ	Symbol for incremental properties
ε	Relative overall strain of column, $\varepsilon = u_G/L$
ε_C	Relative overall strain at local buckling, $\varepsilon_C = \sigma_C / E$
$\bar{\varepsilon}_{\alpha\beta}$	General strain tensor, strain in any materail point
$\varepsilon_{\alpha\beta}$	General membrane strain tensor, strain in any plate middle planes
η	Perturbation parameter, continuously increasing arc length parameter along equilibrium path

η_{BR}	Reduced modulus factor in bending, non-dimensionless, applies for geometrically perfect panels
θ	Relative end-rotation of cross-section ends, positive giving compression in stiffener top, angle rotation of Shanley model
θ_0	Initial relative end-rotation of cross-section ends, imperfection, always positive, initial angle rotation of Shanley model
θ_F	First yield rotation, $\theta_F = \sigma_F L/(Ec_f)$
$\kappa_{\alpha\beta}$	General bending strain tensor of plate middle planes
κ	Relative overall curvature of Shanley model, $\kappa = \theta/L$
κ_0	Relative initial overall curvature of Shanley model, $\kappa_0 = \theta_0/L$
ν	Poisson's ratio
ξ	Non-dimensional global deflection amplitude, $\xi = w_\xi / t_p$
ξ_0	Non-dimensional global imperfection amplitude, $\xi_0 = w_{\xi 0} / t_p$
$\overline{\sigma}_{\alpha\beta}$	General stress tensor, stress in any materail point
$\sigma_{\alpha\beta}$	General membrane stress tensor, stress in any plate middle planes
σ_F	Yield stress
$\overline{\sigma}_x$	Axial membrane stress in each component plate in cross-section, positive in compression
σ_C	Local ideal elastic buckling stress, local eigenvalue
σ_E	Overall ideal elastic buckling stress, global eigenvalue (Euler buckling stress)

Subscripts and superscripts

s	Parameter evaluated at arbitrary state I_s
C	Critical local state I_C , initial buckling in mode q_1 or q_2
0	Geometrically imperfect unloaded state I_0
α	Index for cartesian co-ordinate x_α, α = 1, 2
β	Index for cartesian co-ordinate x_β, β = 1, 2
B	Bending
R	Reduced modulus
$\overline{x}$	A bar over a symbol indicates value evaluated outside the reference plane

Notation for derivatives

$\dot{P}$	First order path derivatives of P ($\dot{P} \equiv \partial P / \partial \eta$)
$\ddot{P}$	Second order path derivatives of P ($\ddot{P} \equiv \partial^2 P / \partial \eta^2$)
$\dot{x}$	First order path derivatives of x ($\dot{x} \equiv \partial x / \partial \eta$), general notation
$\ddot{x}$	Second order path derivatives of x ($\ddot{x} \equiv \partial^2 x / \partial \eta^2$), general notation
$w_{,x}$	First order partial derivatives of w with respect to x ($w_{,x} \equiv \partial w / \partial x$) etc.
V_i	First derivative of potential energy with respect to q_i
V_{ij}	Second derivative of potential energy with respect to q_i and q_j
V_{ijk}	Third derivative of potential energy with respect to q_i and q_j and q_k
$V_{i\varepsilon}$	Second derivative of potential energy with respect to q_i and ε
$V_{i\kappa}$	Second derivative of potential energy with respect to q_i and κ

$V_{ij\varepsilon}$	Third derivative of potential energy with respect to q_i , q_j and ε
$V_{ij\kappa}$	Third derivative of potential energy with respect to q_i , q_j and κ
$\left\|V_{ij}\right\|$	Stability determinant in local modes

Appendix A1 Potential energy of stiffened panel unit - Local modes q_1, q_2

Potential energy $V(\varepsilon, \kappa, q_1, q_2)$ per unit volume $A_T L$ is

$$
\begin{aligned}
&V(\varepsilon, \kappa, q_1, q_2) = \\
&+ a_4 (q_1)^4 \\
&+ a_3 q_{10} (q_1)^3 \\
&+ a_{21} (q_1)^2 + a_{22} (q_{10})^2 (q_1)^2 \\
&+ b_4 (q_2)^4 \\
&+ b_3 q_{20} (q_2)^3 \\
&+ b_{21} (q_2)^2 + b_{22} (q_{20})^2 (q_2)^2 \\
&+ c_4 (q_1)^2 (q_2)^2 \\
&+ c_{31} q_{10} q_1 (q_2)^2 + c_{32} q_{20} q_2 (q_1)^2 \\
&+ c_{21} q_{10} q_{20} q_1 q_2 + c_{22} (q_{20})^2 (q_1)^2 + c_{23} (q_{10})^2 (q_2)^2 \\
&+ g_{1u} (q_1)^2 u + g_{1u0} q_{10} q_1 u + g_{1\theta} (q_1)^2 \theta + g_{1\theta 0} q_{10} q_1 \theta \\
&+ g_{2u} (q_2)^2 u + g_{2u0} q_{20} q_2 u + g_{2\theta} (q_2)^2 \theta + g_{2\theta 0} q_{20} q_2 \theta \\
&+ h_{uu} u^2 + h_{u\theta} u\theta + h_{\theta\theta} \theta^2
\end{aligned}
$$

The geometrical coefficients are given the following symbolisation

a_4 - fourth order q_1 mode
a_3 - third order q_1 mode
a_{21} - second order q_1 mode
a_{22} - second order imperfection q_1 mode

b_4 - fourth order q_2 mode
b_3 - third order q_2 mode
b_{21} - second order q_2 mode
b_{22} - second order imperfection q_2 mode

c_4 - fourth order q_1 q_2 mode
c_{31} - third order imperfection q_1 q_2 mode
c_{32} - third order imperfection q_1 q_2 mode
c_{21} - second order imperfection q_1 q_2 mode
c_{22} - second order imperfection q_1 q_2 mode
c_{23} - second order imperfection q_1 q_2 mode

The energy constants entering the potential energy expression V are defined as

$$a_4 = \frac{E}{2V_{vol}}\left[\frac{3}{128}sLt_p{}^5R_1{}^4D_1{}^4 + \frac{1}{5}HLt_wY_1{}^2 + b_ft_fLY_1{}^2\right]$$

$$a_3 = 4a_4$$

$$a_{21} = \frac{E}{V_{vol}}\left[\begin{array}{l}\frac{1}{96(1-\nu^2)}t_p{}^5LsY_{Y1}R_1{}^2 + \frac{1}{144(1-\nu^2)}t_w{}^5HL(D_1{}^4 + 6(1-\nu)\left(\frac{1}{H}\right)^2 D_1{}^2) \\ +\frac{1}{4}I_ft_w{}^2LD_1{}^4 + \frac{1}{8(1+\nu)}J_p\left(\frac{1}{H}\right)^2 t_w{}^2LD_1{}^2\end{array}\right]$$

$$a_{22} = 4a_4$$

$$b_4 = \frac{E}{2V_{vol}}\left[\frac{3}{128}t_p{}^5sLR_2{}^4D_2{}^4 + \frac{3}{2}HLt_wY_2{}^2\right]$$

$$b_3 = 4b_4$$

$$b_{21} = \frac{E}{V_{vol}}\left[\begin{array}{l}\frac{1}{96(1-\nu^2)}t_p{}^5LsY_{Y2}R_2{}^2 + \frac{1}{96(1-\nu^2)}t_w{}^5HL\left(D_2{}^2 + \left(\frac{\pi}{H}\right)^2\right)^2 \\ +J_pt_w{}^4L\frac{1}{8(1+\nu)}\left(\frac{\pi}{H}\right)^2 D_2{}^2\end{array}\right]$$

$$c_4 = \frac{E}{2V_{vol}}t_psL\left[\begin{array}{l}\frac{3}{64}t_p{}^4D_1{}^2D_2{}^2R_1{}^2R_2{}^2 + \frac{1}{1024}t_p{}^4Y_{22}R_1{}^2R_2{}^2 + \frac{1}{1024}t_p{}^4Y_{33}R_1{}^2R_2{}^2 \\ +HLt_w\left(\frac{2}{3} - \frac{1}{\pi^2}\right)Y_1Y_2\end{array}\right]$$

$$c_{31} = 2c_4$$

$$c_{32} = c_{31}$$

$$c_{21} = \frac{E}{2V_{vol}} t_p sL \left[\begin{array}{l} \frac{12}{64} t_p{}^4 D_1{}^2 D_2{}^2 R_1{}^2 R_2{}^2 + \frac{2}{1024} t_p{}^4 Y_{22} R_1{}^2 R_2{}^2 + \frac{2}{1024} t_p{}^4 Y_{33} R_1{}^2 R_2{}^2 \\ +4HLt_w \left(\frac{2}{3} - \frac{1}{\pi^2} \right) Y_1 Y_2 \end{array} \right]$$

$$c_{22} = \frac{E}{2V_{vol}} t_p Ls \left[\frac{2}{1024} t_p{}^4 Y_{22} R_1{}^2 R_2{}^2 + \frac{2}{1024} t_p{}^4 Y_{33} R_1{}^2 R_2{}^2 \right]$$

$$c_{23} = c_{22}$$

Load coefficients

$$g_{1u} = -\frac{E}{2A_T} \left[\frac{1}{4} t_p s \frac{1}{4} t_p{}^2 D_1{}^2 R_1{}^2 u_F + \frac{2}{3} H t_w{}^2 Y_1 \theta_F + 2 b_f t_f Y_1 u_F \right]$$

$$g_{1u0} = 2 g_{1u}$$

$$g_{1\theta} = \frac{E}{2A_T} \left[t_p s \frac{1}{4} t_p{}^2 D_1{}^2 R_1{}^2 z_G \theta_F - H t_w{}^2 Y_1 \theta_F \frac{1}{12} (3H - 4z_G) - 2 b_f t_f Y_1 \theta_F (H - z_G) \right]$$

$$g_{1\theta 0} = 2 g_{1\theta}$$

$$g_{2u} = -\frac{E}{2A_T} \left[t_p s \frac{1}{4} t_p{}^2 D_2{}^2 R_2{}^2 u_F + 2 H t_w Y_2 u_F \right]$$

$$g_{2u0} = 2 g_{2u}$$

$$g_{2\theta} = \frac{E}{2A_T} \left[t_p s \frac{1}{4} t_p{}^2 D_2{}^2 R_2{}^2 z_G \theta_F - H t_w{}^2 Y_2 \theta_F \frac{1}{2} (H - 2z_G) \right]$$

$$g_{2\theta 0} = 2 g_{2\theta}$$

The h constants are not coupled to the displacement variable q_1 or q_2 and vanish in equilibrium equations. They are therefore of no practical significance are not given here.

Parameters entering the energy constants

$$D_1 = \frac{q\pi}{L}$$
$$D_2 = \frac{p\pi}{L}$$
$$D_3 = \frac{\pi}{s}$$
$$D_4 = \frac{2\pi}{s}$$

$$Y_1 = t_w{}^4 D_1{}^2 / 4$$
$$Y_{21} = t_w{}^4 D_2{}^2 / 8$$
$$Y_{Y1} = (D_1{}^2 + D_3{}^2)^2$$
$$Y_{Y2} = (D_2{}^2 + D_3{}^2)^2$$
$$Y_{22} = \left[\left((q+p)\frac{\pi}{L}\right)^4 D_4{}^8\right] \Big/ \left[\left((q-p)\frac{\pi}{L}\right)^2 + D_4{}^2\right]^4$$
$$Y_{33} = \left[\left((q-p)\frac{\pi}{L}\right)^4 D_4{}^8\right] \Big/ \left[\left((q+p)\frac{\pi}{L}\right)^2 + D_4{}^2\right]^4$$

$$R_1 = \frac{t_w s}{t_p H}\frac{1}{\pi}$$
$$R_2 = \frac{t_w s}{t_p H}$$
$$H = \frac{1}{2}b_f + h_w + \frac{1}{2}t_p$$

$$u_F = \frac{\sigma_F}{E}L$$
$$\theta_F = \frac{\sigma_F}{E}\frac{L}{c_f}$$
$$P_F = \frac{EA_T u_F}{L}$$
$$M_F = \frac{EI_T \theta_F}{L}$$

Appendix A2 First order energy coefficients - Equilibrium equations in local modes q_1, q_2

The principle of stationary potential energy, i.e.

$$\frac{\partial V}{\partial q_1} = 0$$
$$\frac{\partial V}{\partial q_2} = 0$$

gives the following two equilibrium equations as

$$V_1 = 0$$
$$V_2 = 0$$

where the first order energy derivatives V_1 and V_2 is found as

$$V_1 =$$
$$+4a_4(q_1)^3$$
$$+3a_3q_{10}(q_1)^2$$
$$+2a_{21}q_1 + 2a_{22}(q_{10})^2q_1$$

$$+2c_4q_1(q_2)^2$$
$$+c_{31}q_{10}(q_2)^2 + 2c_{32}q_{20}q_2q_1$$
$$+c_{21}q_{10}q_{20}q_2 + 2c_{22}(q_{20})^2q_1$$

$$+2g_{1u}q_1\varepsilon + g_{1u0}q_{10}\varepsilon + 2g_{1\theta}q_1\kappa + g_{1\theta0}q_{10}\kappa$$

$$V_2 =$$
$$+4b_4(q_2)^3$$
$$+3b_3q_{20}(q_2)^2$$
$$+2b_{21}q_2 + 2b_{22}(q_{20})^2q_2$$

$$+2c_4q_2(q_1)^2$$
$$+2c_{31}q_{10}q_1q_2 + c_{32}q_{20}(q_1)^2$$
$$+c_{21}q_{10}q_{20}q_1 + 2c_{23}(q_{10})^2q_2$$

$$+2g_{2u}q_2\varepsilon + g_{2u0}q_{20}\varepsilon + 2g_{2\theta}q_2\kappa + g_{2\theta0}q_{20}\kappa$$

University of Oslo
Department of Mathematics, Mechanics division
Buckling of stiffened Plates using a Shanley model approach

Appendix A3 Single mode equilibrium equation in closed form

The single mode cases

$$\frac{\partial V}{\partial q_1} = 0;\ q_2 = 0 \qquad \text{or} \qquad \frac{\partial V}{\partial q_2} = 0;\ q_1 = 0$$

gives a closed form solution for the equilibrium equations

The case $V_1 = 0$ and $q_2 = 0$ in Appendix A2 is rewritten as

$$-\left[(2g_{1u}q_1 + g_{1u0}q_{10})\varepsilon + (2g_{1\theta}q_1 + g_{1\theta 0}q_{10})\kappa\right] = 2a_{21}q_1\left[1 + \frac{4a_4}{2a_{21}}(q_1^{\,2} + \frac{3a_3}{4a_4}q_1q_{10} + \frac{2a_{22}}{4a_4}q_{10}^{\,2})\right]$$

Using the relation between coefficients given in Appendix A1, i.e.

$$a_3 = 4a_4$$
$$a_{22} = 4a_4$$
$$g_{1u0} = 2g_{1u}$$
$$g_{1\theta 0} = 2g_{1\theta}$$

and substituting these into the equilibrium equation, the following compact form emerge

$$L_\varepsilon\varepsilon + L_\kappa\kappa = \frac{q_1}{q_1 + q_{10}}\left[1 + b_2(q_1^{\,2} + 3q_1q_{10} + 2q_{10}^{\,2})\right]$$

where per definition

$$L_\varepsilon = \frac{g_{1u}}{a_{21}}$$
$$L_\kappa = \frac{g_{1\theta}}{a_{21}} \qquad \varepsilon = u/L \qquad \kappa = \theta/L$$
$$b_2 = \frac{a_4}{a_{21}}$$

The case of only q_2 mode gives a corresponding equilibrium equation in exactly the same form as for the q_1 mode. The coefficients L_ε, L_κ, and b_2 are then defined in terms of the corresponding b and g parameters given in the equilibrium equation $V_2 = 0$.

Appendix A4 Second and third order energy coefficients

Second order energy derivatives

$$V_{11} = +12a_4(q_1)^2 + 6a_3q_{10}q_1 + 2a_{21} + 2a_{22}(q_{10})^2 + 2c_4(q_2)^2 + 2c_{32}q_{20}q_2 + 2c_{22}(q_{20})^2 + 2g_{1u}\varepsilon + 2g_{1\theta}\kappa$$

$$V_{22} = +12b_4(q_2)^2 + 6b_3q_{20}q_2 + 2b_{21} + 2b_{22}(q_{20})^2 + 2c_4(q_1)^2 + 2c_{31}q_{10}q_1 + 2c_{23}(q_{10})^2 + 2g_{2u}\varepsilon + 2g_{2\theta}\kappa$$

$$V_{12} = V_{21} = +4c_4q_1q_2 + 2c_{31}q_{10}q_2 + 2c_{32}q_{20}q_1 + c_{21}q_{10}q_{20}$$

Third order energy derivatives

$$V_{111} = +24a_4q_1 + 6a_3q_{10}$$

$$V_{222} = +24b_4q_2 + 6b_3q_{20}$$

$$V_{112} = V_{211} = V_{121} = +4c_4q_2 + 2c_{32}q_{10}$$

$$V_{221} = V_{122} = V_{212} = +4c_4q_1 + 2c_{31}q_{10}$$

Energy derivatives with respect to q_i and control parameters u and θ

$$V_{1\varepsilon} = 2g_{1u}q_1 + g_{1u0}q_{10}$$

$$V_{1\kappa} = 2g_{1\theta}q_1 + g_{1\theta0}q_{10}$$

$$V_{2\varepsilon} = 2g_{2u}q_2 + g_{2u0}q_{20}$$

$$V_{2\kappa} = 2g_{2\theta}q_2 + g_{2\theta0}q_{20}$$

$$V_{11\varepsilon} = 2g_{1u}$$

$$V_{11\kappa} = 2g_{1\theta}$$

$$V_{22\varepsilon} = 2g_{2u}$$

$$V_{22\kappa} = 2g_{2\theta}$$

$$V_{12\varepsilon} = 0$$

$$V_{12\kappa} = 0$$

Appendix A5 Eigenvalues in local modes

The stability of an equilibrium state is explored by checking the sign of the stability determinant $D = |V_{ij}|$. For the present local two degree of freedom model the stability determinant is

$$D = \begin{vmatrix} V_{11} & V_{12} \\ V_{21} & V_{22} \end{vmatrix} = V_{11}V_{22} - V_{12}^{\,2}$$

A positive value indicates a stable equilibrium state while a negative value indicates an unstable equilibrium state.

For classical eigenvalue calculations the stability of the perfect flat form is to be investigated, i.e. the energy coefficients V_{ij} is to be evaluated for

$$q_1 = 0$$
$$q_2 = 0$$
$$q_{10} = 0$$
$$q_{20} = 0$$

From the expressions given in Appendix A4 this gives the following condition for initial buckling of the flat plate into the local buckling modes

$$D = \begin{vmatrix} V_{11} & 0 \\ 0 & V_{22} \end{vmatrix} = V_{11}V_{22} = 0$$

which have two solutions

$$V_{11} = 0$$
$$V_{22} = 0$$

This means that the eigenvalues in the two local modes are not coupled. For the case of pure uni-axial compression, i.e. $\kappa = 0$ is prescribed, the eigenvalues for uni-axial shortening are found as

$$\varepsilon_{C1} = -\frac{g_{1u}}{a_{21}}$$
$$\varepsilon_{C2} = -\frac{g_{2u}}{b_{21}}$$

with corresponding nominal buckling stresses $\sigma_{C1} = E\varepsilon_{C1}$, $\sigma_{C2} = E\varepsilon_{C2}$

in mode q_1 and q_2 respectively. In the present two-degree of freedom model the eigenvalue in each mode is minimised with respect to the wave buckling parameter q and p respectively.

Appendix A6 Macro material coefficients – Local compatibility conditions

The load-shortening-deflection amplitude relations are

$$N(\varepsilon,\kappa,q_1,q_2) = K_{11}{}^{L}\varepsilon + K_{12}{}^{L}\kappa + B_{11}(q_1^2 + 2q_1q_{10}) + B_{12}(q_2^2 + 2q_2q_{20})$$
$$M(\varepsilon,\kappa,q_1,q_2) = K_{21}{}^{L}\varepsilon + K_{22}{}^{L}\kappa + B_{21}(q_1^2 + 2q_1q_{10}) + B_{22}(q_2^2 + 2q_2q_{20})$$

The linear constants are defined as

$$K_{11}{}^{L} = EA_T$$
$$K_{12}{}^{L} = 0$$
$$K_{21}{}^{L} = 0$$
$$K_{22}{}^{L} = EI_T$$

where A_T is the total cross-sectional area and I_T is the moment of inertia about the centroid of the cross-section of one unit consisting of one stiffener with associated full plate width. The $K_{12}{}^{L} = K_{21}{}^{L}$ coefficients are zero since the stiffness properties are calculated about the centroid of the cross-section.

The geometrical constants coupled to the non-linear cross-sectional buckling modes q_1 and q_2 are defined as

$$B_{11} = -\frac{E}{4}t_w{}^2\left(\frac{\pi q}{L}\right)^2\left[\frac{1}{3}\frac{t_w}{H^2}\left((h_w+\frac{t_p}{2})^3-\left(\frac{t_p}{2}\right)^3\right)+b_f t_f\right]-\frac{E}{8}t_w{}^3 sR_1{}^2\left(\frac{\pi q}{L}\right)^2$$

$$B_{12} = -\frac{E}{4}t_w{}^3\left(\frac{\pi p}{L}\right)^2 h_w - \frac{E}{8}t_p{}^3 sR_2{}^2\left(\frac{\pi p}{L}\right)^2$$

$$B_{21} = -\frac{E}{4}t_w{}^3\left(\frac{\pi q}{L}\right)^2\left[\frac{1}{4}\frac{1}{H^2}\left((h_w+\frac{t_p}{2})^4-\left(\frac{t_p}{2}\right)^4\right)-\frac{1}{3}\frac{z_G}{H^2}\left((h_w+\frac{t_p}{2})^3-\left(\frac{t_p}{2}\right)^3\right)\right]$$
$$-\frac{E}{4}t_w{}^2\left(\frac{\pi q}{L}\right)^2(H-z_G)b_f t_f+\frac{E}{8}t_p{}^2\left(\frac{\pi q}{L}\right)^2 R_1{}^2 z_G t_p s$$

$$B_{22} = -\frac{E}{8}t_w{}^3\left(\frac{\pi p}{L}\right)^2\left[\frac{1}{2}\left((h_w+\frac{t_p}{2})^2-(\frac{t_p}{2})^2\right)-z_G h_w\right]-\frac{E}{8}t_p{}^2 sR_2{}^2\left(\frac{\pi p}{L}\right)^2 z_G t_p$$

The integers q and p are the wave number that minimise the local eigenvalue in the q_1 and q_2 mode respectively.

University of Oslo
Department of Mathematics, Mechanics division

Appendix A7 Macro material coefficients – Solution for perfect geometry

Single mode solution in q_1 mode

$$K_{11} = K_{11}^{\,L} - \frac{1}{2} B_{11} \frac{g_{1u}}{a_4}$$

$$K_{12} = -\frac{1}{2} B_{11} \frac{g_{1\theta}}{a_4}$$

$$K_{21} = -\frac{1}{2} B_{21} \frac{g_{2u}}{a_4}$$

$$K_{22} = K_{22}^{\,L} - \frac{1}{2} B_{21} \frac{g_{1\theta}}{a_4}$$

Single mode solution in q_2 mode

$$K_{11} = K_{11}^{\,L} - \frac{1}{2} B_{12} \frac{g_{2u}}{b_4}$$

$$K_{12} = -\frac{1}{2} B_{12} \frac{g_{2\theta}}{b_4}$$

$$K_{21} = -\frac{1}{2} B_{22} \frac{g_{2u}}{b_4}$$

$$K_{22} = K_{22}^{\,L} - \frac{1}{2} B_{22} \frac{g_{2\theta}}{b_4}$$

Coupled solution in mode q_1 and q_2

$$K_{11} = K_{11}^{\,L} - \left[\frac{B_{11}}{4a_4 - c_4^2/b_4} \left(\frac{c_4}{b_4} g_{2u} - 2g_{1u}\right) + \frac{B_{12}}{4b_4 - c_4^2/a_4} \left(\frac{c_4}{a_4} g_{1u} - 2g_{2u}\right) \right]$$

$$K_{12} = -\left[\frac{B_{11}}{4a_4 - c_4^2/b_4} \left(\frac{c_4}{b_4} g_{2\theta} - 2g_{1\theta}\right) + \frac{B_{12}}{4b_4 - c_4^2/a_4} \left(\frac{c_4}{a_4} g_{1\theta} - 2g_{2\theta}\right) \right]$$

$$K_{21} = -\left[\frac{B_{21}}{4a_4 - c_4^2/b_4} \left(\frac{c_4}{b_4} g_{2u} - 2g_{1u}\right) + \frac{B_{22}}{4b_4 - c_4^2/a_4} \left(\frac{c_4}{a_4} g_{1u} - 2g_{2u}\right) \right]$$

$$K_{22} = K_{22}^{\,L} - \left[\frac{B_{21}}{4a_4 - c_4^2/b_4} \left(\frac{c_4}{b_4} g_{2\theta} - 2g_{1\theta}\right) + \frac{B_{22}}{4b_4 - c_4^2/a_4} \left(\frac{c_4}{a_4} g_{1\theta} - 2g_{2\theta}\right) \right]$$